

AD-A195 964

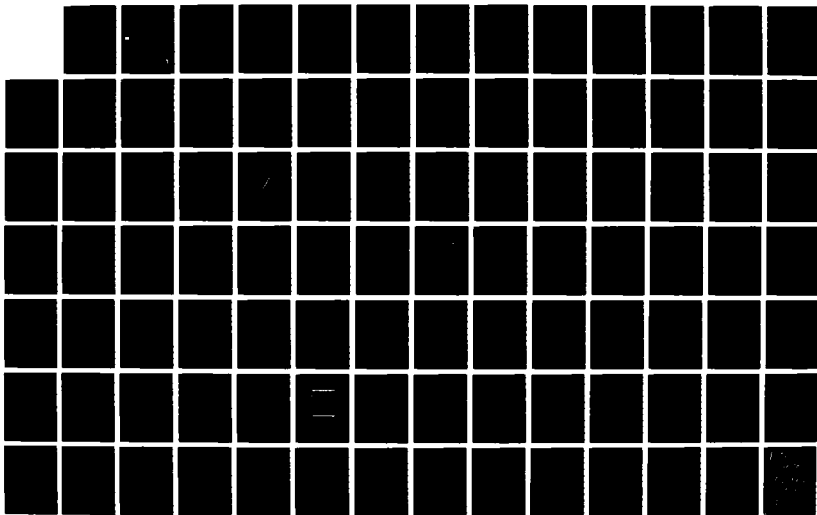
DESIGN OF A COMBINED EFFECTS SIMULATOR(U) CALIFORNIA
RESEARCH AND TECHNOLOGY INC ALBUQUERQUE NM
E J RINEHART ET AL. MAY 88 AFML-TR-87-67

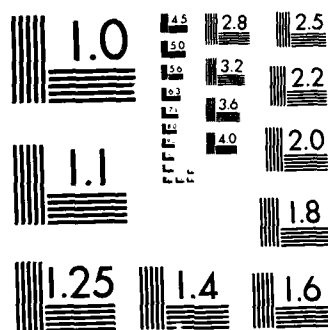
1/1

UNCLASSIFIED F29681-85-C-0004

F/G 19/11

NL





MICROCOPY RESOLUTION TEST CHART
NATIONAL BUREAU OF STANDARDS-1963-A

DTIC FILE COPY

2

AFWL-TR-87-67

AFWL-TR-
87-67

AD-A195 964

DESIGN OF A COMBINED EFFECTS SIMULATOR

E. J. Rinehart
J. R. Rocco
J. M. Thomsen

California Research & Technology, Inc.
2017 Yale Blvd, SE
Albuquerque, NM 87106

May 1988

Final Report

Approved for public release; distribution unlimited.

THIS RESEARCH WAS SPONSORED BY THE DEFENSE NUCLEAR AGENCY UNDER
SUBTASK: RSRD, WORK UNIT: 00121, WORK UNIT TITLE: SIMULATION
DEVELOPMENT.

AIR FORCE WEAPONS LABORATORY
Air Force Systems Command
Kirtland Air Force Base, NM 87117-6008

DTIC
ELECTE
JUN 07 1988

E

88 6 3 077

This final report was prepared by the California Research & Technology, Inc., Albuquerque, New Mexico, under contract F29601-85-C-0004, with the Air Force Weapons Laboratory, Kirtland Air Force Base, New Mexico. Captain William A. Kitch, AFWL/NTED, was the Laboratory Project Officer-in-Charge.

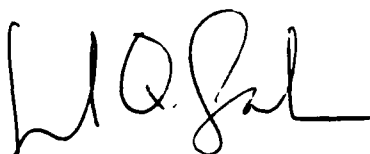
When Government drawings, specifications, or other data are used for any purpose other than in connection with a definitely Government-related procurement the United States Government incurs no responsibility nor any obligation whatsoever. The fact that the Government may have formulated or in any way supplied the said drawings, specifications, or other data, is not to be regarded by implication or otherwise in any manner construed, as licensing the holder or any other person or corporation; or as conveying any rights or permission to manufacture, use, or sell any patented invention that may in any way be related thereto.

This report has been authored by a contractor of the United States Government. Accordingly, the United States Government retains a nonexclusive, royalty-free license to publish or reproduce the material contained herein, or allow others to do so, for the United States Government purposes.

This report has been reviewed by the Public Affairs Office and is releasable to the National Technical Information Service (NTIS). At NTIS, it will be available to the general public, including foreign nationals.

If your address has changed, if you wish to be removed from our mailing list, or if your organization no longer employs the addressee, please notify AFWL/NTED, Kirtland AFB, NM 87117-6008 to help us maintain a current mailing list.

This technical report has been reviewed and is approved for publication.



JUVENAL Q. SALOMON
A1C, USAF
Project Officer



FREDERICK M. JONAS
Lt Col, USAF
Chief, Technology Branch

FOR THE COMMANDER



CARL L. DAVIDSON
Col, USAF
Chief, Civil Engineering Rsch Div

DO NOT RETURN COPIES OF THIS REPORT UNLESS CONTRACTUAL OBLIGATIONS OR NOTICE ON A SPECIFIC DOCUMENT REQUIRES THAT IT BE RETURNED.

REPORT DOCUMENTATION PAGE				
1a. REPORT SECURITY CLASSIFICATION Unclassified		1b. RESTRICTIVE MARKINGS		
2a. SECURITY CLASSIFICATION AUTHORITY		3. DISTRIBUTION / AVAILABILITY OF REPORT		
2b. DECLASSIFICATION / DOWNGRADING SCHEDULE		Approved for public release; distribution unlimited.		
4. PERFORMING ORGANIZATION REPORT NUMBER(S)		5. MONITORING ORGANIZATION REPORT NUMBER(S) AFWL-TR-87-67		
6a. NAME OF PERFORMING ORGANIZATION California Research and Technology, Inc.	6b. OFFICE SYMBOL (If applicable)	7a. NAME OF MONITORING ORGANIZATION Air Force Weapons Laboratory		
6c. ADDRESS (City, State, and ZIP Code) 2017 Yale Boulevard, SE Albuquerque, New Mexico 87106		7b. ADDRESS (City, State, and ZIP Code) Kirtland Air Force Base, New Mexico 87117-6008		
8a. NAME OF FUNDING / SPONSORING ORGANIZATION Defense Nuclear Agency	8b. OFFICE SYMBOL (If applicable)	9. PROCUREMENT INSTRUMENT IDENTIFICATION NUMBER F29601-85-C-0004		
8c. ADDRESS (City, State, and ZIP Code) Washington, DC 20305		10. SOURCE OF FUNDING NUMBERS		
		PROGRAM ELEMENT NO 62715H	PROJECT NO. WDNS	TASK NO 95
		WORK UNIT ACCESSION NO 11		
11. TITLE (Include Security Classification) DESIGN OF A COMBINED EFFECTS SIMULATOR				
12. PERSONAL AUTHOR(S) Rinehart, E. J.; Rocco, J. R.; Thomsen, J. M.				
13a. TYPE OF REPORT Final	13b. TIME COVERED FROM 12/84 TO 09/87	14. DATE OF REPORT (Year, Month, Day) 1988, May	15. PAGE COUNT 96	
16. SUPPLEMENTARY NOTATION THIS RESEARCH WAS SPONSORED BY THE DEFENSE NUCLEAR AGENCY UNDER SUBTASK: RSRD, WORK UNIT: 00121, WORK UNIT TITLE: SIMULATION DEVELOPMENT.				
17. COSATI CODES			18. SUBJECT TERMS (Continue on reverse if necessary and identify by block number)	
FIELD	GROUP	SUB-GROUP	DIHEST Nuclear Simulation	
20	08		HEST Ground Shock	
20	04		CDC-2 Combined Effects	
19. ABSTRACT (Continue on reverse if necessary and identify by block number)				
<p>→ A methodology for designing simulators to model the combined effects of both airblast induced and direct induced ground shock is presented. The report describes how to combine the HEST and DIHEST to make a combined effects simulator.</p> <p>In addition to discussing a general methodology, the report describes how a specific combined effects simulator (CDC-2) was designed. → to p1</p>				
20. DISTRIBUTION / AVAILABILITY OF ABSTRACT <input checked="" type="checkbox"/> UNCLASSIFIED/UNLIMITED <input type="checkbox"/> SAME AS RPT <input type="checkbox"/> DTIC USERS			21. ABSTRACT SECURITY CLASSIFICATION Unclassified	
22a. NAME OF RESPONSIBLE INDIVIDUAL Captain William A. Kitch			22b. TELEPHONE (Include Area Code) (505) 846-6479	22c. OFFICE SYMBOL NTD

UNCLASSIFIED

SECURITY CLASSIFICATION OF THIS PAGE

UNCLASSIFIED

SECURITY CLASSIFICATION OF THIS PAGE

TABLE OF CONTENTS

	<u>Page</u>
INTRODUCTION	1
SCOPE	4
SIMULATION CRITERIA	5
DRY SITE	9
WET AND LAYERED SITES	11
HISTORICAL REVIEW	14
ACID/BUTTERFLY MAIDEN.....	16
DESIGN PROCEDURE FOR A SPECIFIC CASE	21
NUCLEAR ENVIRONMENT	21
INITIAL DESIGN	27
DESIGN PROCEDURES FOR CES IN DRY SOIL	44
GENERAL	44
CALCULATIONAL MODELING	47
CALCULATIONAL SERIES	49
DIHEST	51
EMPIRICAL RESULTS	72
OUTSTANDING TECHNICAL ISSUES	81
SUMMARY OF DESIGN PROCEDURES	83
INTRODUCTION	83
STEP 1. THE NUCLEAR CRITERIA	83
STEP 2. THE PARTS REQUIRED	84
STEP 3. GEOMETRICAL LAYOUT	84
STEP 4. EXPLOSIVE ESTIMATES	85
REFERENCES.....	86



Accession For	
NTIS GRA&I	<input checked="" type="checkbox"/>
DTIC TAB	<input type="checkbox"/>
Unannounced	<input type="checkbox"/>
Justification	
By _____	
Distribution/ _____	
Availability Codes	
_____ and/or _____	
Dist _____	
A-1	

LIST OF FIGURES

<u>Number</u>		<u>Page</u>
1	Nuclear environment for dry site (1 Mt).....	6
2	Early-time free-field environmental histories at the 2-kbar range 58 m below the surface for a 1-Mt surface burst calculation over the less beneficial site (wet/layered).....	7
3	ACID test-bed with hand calculated nuclear explosive crater.....	17
4	PRETEST PREDICTIONS and recorded waveforms for the CES ACID.....	19
5a&b	Nuclear environment to which the CDC series was designed.....	22
5c	Concluded.....	23
6	Horizontal and vertical particle velocity at the 13.9-m (75-ksi) range from the CRT 2-kt RM1 calculation (dry alluvium).....	28
7	Generic conception of the CES simulator.....	29
8	Initial design criteria for the HEST.....	30
9	Plan view of simple HEST design for CDC-2, 96-kt, showing discrete 4- x 8-ft panels.....	32
10	Effects of changing parameters in DIHEST design....	37
11	Effect of HEST on DIHEST free-field motions for Pre-CARES.....	40
12	Effect of depth of burial of DIHEST on vertical velocity gradient.....	42
13	Cross section of CDC-2.....	43
14	Profile view of combined effects simulator test-bed.....	45
15	Modeling of the DIHEST for the calculations.....	50
16	Peak horizontal velocity versus range for DIHEST only.....	52

LIST OF FIGURES (continued)

<u>Number</u>		<u>Page</u>
17	Peak overpressure of airblast versus nuclear range for 225-kt nuclear surface burst.....	54
18	NMERI parametric series.....	55
19	Comparison of DIHEST-only and CES calculations 3 and 4 with respect to peak horizontal velocity and DIHEST centerline.....	56
20	Peak horizontal stresses for the DIHEST-only (calculation 2a) and two CES cases (3 and 4).....	58
21	Comparison of waveforms for the DIHEST only and four CES (3, 4, 5, and 16).....	60
22	Peak horizontal velocities for calculations 2c (DIHEST-only), 5, and 6 (CES).....	62
23	Parameter study for combined effects simulator.....	64
24a	Pre-CARES 2 crater profile along DIHEST centerline, and preshot and postshot gage locations for gages within 0.5 m of the centerline.....	66
24b	Pre-CARES 2 crater profile through the HEST centerline, parallel to the DIHEST at range = 6 m, and pretest and posttest gage locations for gages within 1 m of this line.....	66
25	Horizontal velocity waveforms in the combined effects region (CDC-1).....	68
26	Horizontal velocity histories at the 16.0 m range (344 MPa) measured in CDC-1.....	69
27	Cross section of the crater produced by CDC-1.....	71
28	Waveform comparison of unHESTed and HESTed velocity waveforms.....	74
29	CES cross section and resulting peak DIHEST velocities.....	76
30	Comparison of peak velocities of the DI wave with airblast subtracted.....	78
31	ACID test.....	79

CONVERSION FACTORS, NON-SI TO SI (METRIC)
UNITS OF MEASUREMENT

Non-SI units of measurement used in this report can be converted to SI (metric) units as follows:

<u>Multiply</u>	<u>By</u>	<u>To Obtain</u>
degrees (angle)	0.01745329	radians
feet	0.3048	meters
gallons (US liquid)	3.785412	cubic decimeters (liters)
inches	2.54	centimeters
kips (force)	4.448222	kilonewtons
kips (force per square inch)	6.894757	megapascals
megatons (nuclear equivalent of TNT)	4.184	petajoules
pounds (force) per square inch	6.894757	kilopascals
pounds (mass)	0.4535924	kilograms
pounds (mass) per cubic foot	16.01846	kilograms per cubic meter
kbars	98	megapascals
feet	1/.3048	meters

1473
INTRODUCTION

→ A Combined Effects Simulator (CES) is an array of high explosives that has been designed to simulate, in a prescribed manner, the total nuclear environment either at a particular point, as in this report, or in a global sense as CARES simulators do. → The nuclear environment can be conveniently broken down into three basic components; each component is usually simulated with a particular type of simulator and, thus, the CES is truly a combination of both effects and simulators. (Ref. 1). The effects and most common simulator used to produce the effects are:

1. → LOCAL AIRBLAST. The local airblast refers to the peak values and waveforms created, at a specific point on the surface, by the airblast wave generated in a near surface explosion. For near surface structures, the local airblast generally dictates the vertical motions and both the maximum horizontal and vertical stresses. The local airblast is usually simulated with the High Explosive Simulation Technique (HEST).
2. → UPSTREAM AIRBLAST. The upstream airblast refers to the energy put into the ground nearer the source than the local airblast. It has been recently associated with the crater-related wave discussed below in 3; however, it is separated here because it has been in the past usually simulated with a HEST or Berm Loaded Explosive Simulation Technique (BLEST) not in juxtaposition with the HEST used for the local airblast.
3. → SOURCE-INDUCED MOTIONS, (DIHEST). The source-induced (SI) motions include both the direct-induced (DI) wave (energies directly deposited near the nuclear source) and the crater-related wave (resulting from the crater growth and stopping and the upstream airblast).

Simulation of the SI wave is done with the Direct-Induced High Explosive Simulation Technique (DIHEST). Since, near the surface, the largest stress is related to the airblast loading, the emphasis has been on horizontal SI motions only, neglecting the corresponding stresses.

Usually, only one type of simulator is used for testing a particular component. For example, silo headworks have been tested against local vertical airblast loadings using a HEST. Horizontal rattle space is tested using a DIHEST. As higher overpressures were investigated, it became clear that the vertical local airblast motions and the horizontal DI motions affected each other so that the combination of the two into a single CES was necessary.

The experimental data from which to develop a design procedure for a generic CES are very limited, with only three recent test series available. These include the ACID-BUTTERFLY MAIDEN (1/4-scale of 100 kt at the 3-ksi overpressure range), Pre-CARES (2 kt at the 100-ksi range), and the Combined DIHEST Calibration (CDC) series (12 to 96 kt at ranges corresponding to 30 to 80 ksi). All of the CES designed to date have been a combination of a HEST and DIHEST (either a planar array of drill holes, sheet charges or central charge). The general physics of the simulator is understood; however, details of such parameters as precompaction or spall of the test-bed by the HEST, spatial locations of the simulator parts, initiation schemes, burn rates, aspect ratios, etc., are not well in hand for other than the few specific cases tested. In fact, many design parameters used in CES were decided upon apparent feasibility rather than scientific or engineering considerations. When a design is desired, presently a rough conceptual plan based on the limited data base is developed and tested calculationaly with limited parametric studies being available. Thus, any design that is beyond the

rather limited data base must be well calculated and tested, probably at smaller scale before any certainty can be placed upon its expected output.

SCOPE

To gain an understanding of what is required for the design of a true combined effects simulator, the components that make up the nuclear waveform are discussed. By understanding where specific waves come from in the free field, a better understanding of what types of explosive arrays and their respective placement to the simulation area will be obtained.

Following the description of the problem, a short historical review of previous test series is presented to give an appreciation of simulator parts and problems associated with their combination to produce a combined effects waveform. Tests are identified and good points, along with pitfalls, are discussed.

Details of the most recently designed and fielded combined effects simulation, the CDC series, are described in detail. This discussion will give the user the ability to design with some confidence a simulator that in dry soil will produce motions resulting from a 2- to 96-kt nuclear surface burst for ranges corresponding to 30- to 100-ksi peak overpressures.

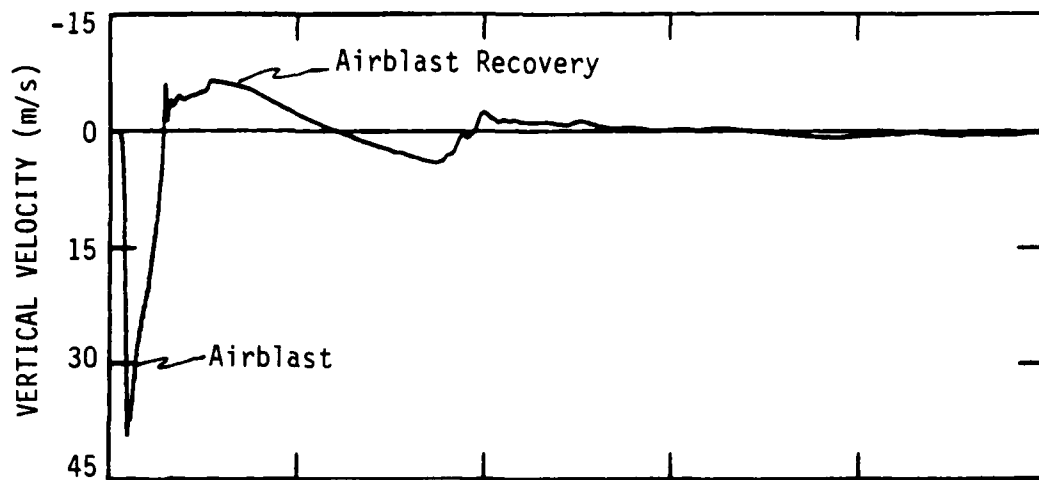
Finally, a general design concept will be presented using results of a limited parameter study. It must be understood that there are a limited number of test-bed designs and, if the user desires to extend the procedures to new sites and environments of interest, rather extensive additional work will be necessary to assure the success of the simulator.

Many concepts are discussed that have to do with details of both nuclear environments and simulation design and fielding, with which it is assumed the user is familiar. Good short discussions of both nuclear environments and simulator design and simulation of the environment are contained in Reference 2 (Chapters 4, 5, 6 and 7).

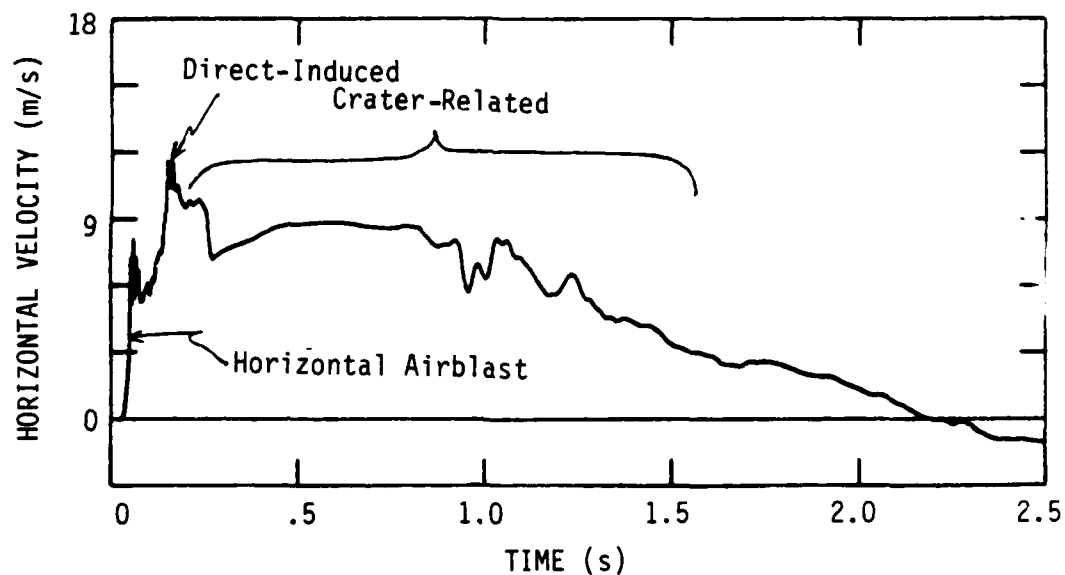
SIMULATION CRITERIA

The concept for an initial design for any CES comes from understanding in detail the nuclear environment that is required. By understanding the environment and its importance to the test structure, the simulation criteria can be developed. The simulation criteria is a statement telling what portion of the actual nuclear environment must be modeled; that is, what motion and stresses as a function of space and time must be produced by the simulator. The criteria are based on the nuclear environment, but must consider: what is important to the structure behavior, what can reasonably be measured, and what uncertainties exist in the environment. The criteria sets not only expectations for a simulator but also the basis for evaluating the results of a test. The criteria are oftentimes given as a peak value obtained at a specific time (e.g., 0.6-m displacement at 300 ms); however, CESs have generally been designed to meet entire time histories of velocities and vertical stresses. Before a complete design can be completed, the criteria, and their origin, must be understood in detail.

Figures 1 and 2 show typical nuclear environment waveforms that might be simulated. Figure 1 contains the vertical and horizontal velocity histories for a typical homogeneous, dry site. The CDC series was designed for such a site. Designs for CES tests can, with some assurance, be used in the future for this type of site. Figure 2 shows the vertical and horizontal velocity waveforms for a typical wet layered site having a dry upper layer, near surface water table, and a deeper rock layer. Combined effects simulators have not yet been designed or tested for this type of geology; however, by understanding where the various parts of the total waveform come from, one can understand what is required for a CES design.

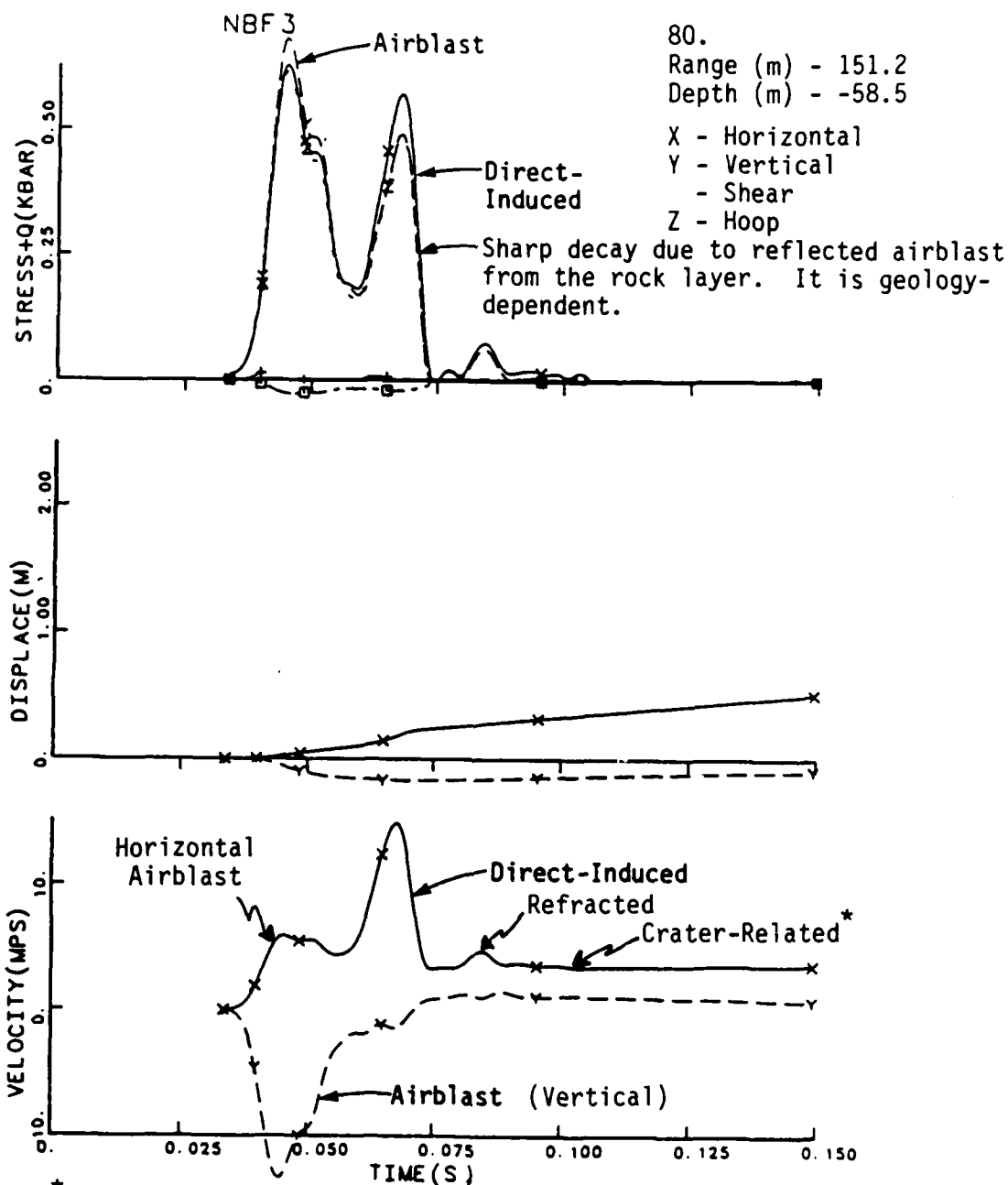


(a) Vertical velocity, 22-m depth, 177-m range.



(b) Horizontal velocity, 22-m depth, 177-m range.

Figure 1. Nuclear environment for dry site (1 Mt).



* Note the extremely long duration of the crater-related.

Figure 2. Early-time free-field environmental histories at the 2-kbar range 58 m below the surface for a 1-Mt surface burst calculation over the less beneficial site (wet/layered).

Two terms related to simulation and simulation criteria must be defined. They are:

1. Fidelity. The fidelity of a simulator tells how well it matches the nuclear environment. The higher the fidelity, the more nuclearlike the simulation.
2. Simulation Time (t_s). This is the duration for which the simulator provides the proper environment to the test articles; in other words, it is the time that the test article could not differentiate between a true nuclear environment and the simulation. The primary reason a simulator loses its fidelity is arrival of effects from its finite edges. General considerations of structural response show that airblast simulation times are smaller, by as much as an order of magnitude, than the duration of the usual SI wave. The upper portion of a silo, for example, is sensitive to the stresses generated in the ground. These are usually at a maximum during the airblast loading. After the short airblast simulation times have been met (impulse criteria), the airblast-induced motions continue to be applied to the structure. Some structure, or internal equipment, components may be motion sensitive. A missile silo shock isolation system (SIS) is sensitive to the maximum displacement, for example. In dry soil, the stresses occurring with the SI motions are small compared to the initial airblast-induced stresses. Therefore, accurate simulation of the SI stresses is not overly important as long as they are less than the initial airblast-induced stresses and do not control system response. In wet layered geologies, the nuclear-generated stresses associated with the DI portion of the SI wave are very important and can exceed the AI stresses. In these cases accurate stress simulation cannot be given up.

Both simulation time t_s and fidelity may be cost drivers. Higher fidelity and longer times inherently imply higher costs. Ultimately, these two items are controlled by the criteria, again showing the importance of setting these is a meaningful way.

DRY SITE (e.g., Yuma, AZ; Fig. 1), SURFACE BURST

Vertical velocity and vertical and horizontal stresses observed in a dry site at ranges corresponding to 30 to 100 ksi are dominated by the vertical airslap. This portion of the simulation can be done well by using a vertical airblast simulator. Of course, the simulation time, fidelity of the simulator, depth of interest, etc., will determine the particular type of simulator that should be used. References 3 and 4 discuss these types in some detail. Reference 2 gives a good overview of advantages and disadvantages of each type. Note in Figure 1, the vertical airslap is the first to arrive at any position; thus, the airblast simulator is the first piece of the CES to work on. The HEST design developed may be used almost directly with little modification required because of the added parts.

The horizontal waveform is more complicated than the vertical. The various peaks and troughs are associated with known sources as indicated in Figure 1. The initial peak is induced by the airblast and is its horizontal component. Basically, it can be ascribed to two different mechanisms: (1) the gradient of overpressure decay observed between the source and the point of interest (the overpressure is monotonically decreasing away from the source), and (2) the difference between the velocity of the airblast traveling along the surface and the ground shock traveling through the earth. If the airblast simulator can be designed to properly replicate the nuclear overpressure including its propagation velocity and pressure gradient, the horizontal airblast should be correct. Because

pressure gradient and velocity differences are required, more than a local airblast simulator is needed. Following closely after the horizontal airblast is the source-induced wave. In the case of dry material only, the crater-related portion predominates. At this range of interest, the direct wave tends to become an integral part of the crater-related wave. These two signals are caused by the energy directly coupled at or near the source, the upstream airblast, and the crater growth and stoppage of that growth. For the simulation of the source-induced waveform the DIHEST has been successful. Note that the source-induced wave is not a first arrival and is affected by the airblast-induced ground shock. This is also true of the DIHEST-produced wave. One cannot simply add a DIHEST waveform to the HEST waveform. The interaction of the two waveforms must be accounted for.

Thus, through an understanding of the nuclear environment, a simulator design can be conceived. Two simulator types are used to simulate the two basic waves seen in the environment--the HEST for the airblast and the DIHEST for the source-induced motions. The first arrival is from the airblast so the HEST can be used without considering any alteration from the DIHEST. Some degree of confidence in the late-time performance of the HEST (i.e., beyond the airblast simulation time) is required. Impulse delivered at times corresponding to SI wave simulation should be close to the late-time nuclear airblast impulse. Relief effects of HEST edges also need to be considered. It needs to be assumed, for example, that the airblast-induced motions are not greatly affected by the test-bed edges during the time of the CES simulation. On the other hand, the source-induced motions, or those simulated by the DIHEST, are affected by the HEST. Almost all of the DIHEST data used for design are based on DIHEST only tests and, therefore, should not be used directly without consideration of how the HEST changes the site material and the motions and stresses. In dry material, substantial crush-up of

the test-bed occurs, changing material properties that the DIHEST waves will travel through; thus requiring alteration of the DIHEST-only experimental data when used in the CES.

WET AND LAYERED SITES (e.g., Silo Test Program (STP); Fig. 2)

Figure 2 shows the nuclear environment calculated for a layered site that contains a dry, thin near-surface layer, a saturated soil layer, and a deeper saturated weak rock layer. The main difference between the saturated soil and rock is strength. Details of a CES design have not been worked out in any detail for this type of environment, but through an understanding of the nuclear environment, initial suggestions for parts of the CES and their combination can be considered.

As before, the airblast-induced ground shock arrives first and should be modeled using the usual airblast simulators. HEST and BLEST designs are presently straightforward; however, for wet and layered sites there is not as extensive a data base as there is for dry homogeneous sites. For example, the later-time reflections from the water table and rock layer tend to reduce the downward vertical velocities and displacements. Since these times are of interest in a typical CES-type simulator, they must be considered in the design of the airblast simulator. However, it is not clear whether or not they can be adequately modeled with a finite-sized HEST/BLEST combination. This question must be addressed through calculations of the simulator design.

Horizontal motions associated with the wet/layered site are substantially different from those of the dry site. Initial motion is again associated with the vertical airblast and should be modeled by the HEST/BLEST. But at that point the similarity stops. The wet/layered site is not like the dry site where the crater-related and direct wave form a source-induced wave with a single pulse. As Figure 2 shows, the wet/layered SI wave

contains a short direct pulse followed by a very long CR pulse. These two different features of the SI wave cannot be modeled by a single DIHEST. One possible technique would be to model the short direct pulse with a single charge and use a DIHEST to give the CR pulse. Figure 2 also shows a refracted wave adding to the horizontal motion. In this case it is small, but in other geologies it could be much larger. In the past, this motion has been simulated not with a DIHEST but with a far-field airblast simulator.

The wet or layered case appears to be more difficult to understand and simulate than the dry homogeneous site. Concepts for CES in these sites are easy to develop; however, actual designs must be determined by calculations as no data exist. One advantage of wet sites is that superposition of waveforms from simulator parts will probably give acceptable estimates of the performance of the entire simulator, because the material is more elastic than in the dry case.

With these simple examples, it should be clear that the nuclear waveform will dictate the parts to be used in a CES. Also, by understanding which part can be associated with which wave, an understanding of the limited CES data base can now be looked at.

In summary, before a design for a CES can be estimated, criteria must be set, specifying what part of the nuclear environment must be modeled. The criteria must include the requirements of what is to be simulated (e.g., vertical airslap, crater-related, etc.), for how long, with what precision, and acceptable deviations. Only after the criteria are set can a simulator be suggested. For example, if a good simulation of the airslap is required followed only by a peak horizontal displacement, then a well-designed HEST and a single charge placed to give only peak displacements is required. If, on the

other hand, the histories of both the vertical and horizontal velocities are required to be simulated to within $\pm 20\%$, a HEST and well-designed and -placed DIHEST array are suggested. In the second case, much more care will have to be taken in the design, including calculational iterations and possible small-scale pretest shots. The criteria are then the key, and the details of the CES are described by that criteria.

HISTORICAL REVIEW

The initial concept of combining a HEST and DIHEST simulator to produce both vertical and horizontal direct-induced and airblast loadings was proposed and tested in the late 1960s. The ROCK TEST series tested hardened silos drilled into hard rock. Both vertical and horizontal response was evaluated (Ref. 5). The simulator performed adequately but resulted in motions and failures that were not well understood at the time, so the concept was dropped. The next test that required horizontal motions was the HARD PAN series. It was determined that horizontal, upstream airblast refracted by the lower, higher velocity layers was important (Ref. 6). The required upstream-induced airblast was simulated with a BLEST placed beyond the local HEST simulator. Both the ROCK TEST and HARD PAN have little impact on the design in this report and are not discussed further.

The ACID/BUTTERFLY MAIDEN series (Ref. 7) are the first tests that were important to the CDC design effort. The object of these tests was to model both the vertical airslap and SI motions produced by a tactical nuclear weapon. They form a rudimentary basis for the design of true CES simulators. This series was the first attempt to combine a HEST and DIHEST in an alluvial site. The overpressure was modest (24 MPa) and only vertical airslap and crater-related motions were modeled. This test will be discussed further because it has implications concerning the use of a variable pressure HEST and the effect of trying to propagate the crater-related motions and stresses through material that is altered by an airblast simulator.

Another simulation program similar to the ACID test was the SSTM V test recently fired (Ref. 8). Again, this test used simple superposition of separately derived parts (HEST and DIHEST). An understanding of the integration into a reliable combined effects

simulation was not required for the success of the program and thus was neither understood or accounted for.

The most important series is the CDC series. Unlike ACID or SSTM V, CDC was designed by understanding the interaction of all explosive arrays rather than simply superimposing separate pieces. In this sense it was the first true combined effects simulator. Specific details of this test series are discussed in Section 4, and include (1) the preliminary work done with Pre-CARES for selecting an appropriate type of simulator, and (2) the total design of CDC-2, which simulated ground motions at a range corresponding to 550 MPa (80 ksi) overpressures of a 96-kt nuclear surface burst.

Finally, limited work was done for a wet and layered site using the combination of an HEST and a central charge (rather than a DIHEST) to produce the horizontal motions (Ref. 9). This effort pointed out the importance of using calculations when designing a combined effects simulator to simulate an entirely new environment. This particular design followed procedures developed from the CDC experience, but the lack of empirical data, understanding of the environment, and integration of the HEST and central charge via calculations led to a low fidelity simulator.

These few tests constitute the entire combined effects simulator data base, from which new tests and designs can be developed. With the exception of the CDC series, all of the CESSs have been designed with superposition principles. CDC tests were designed using finite difference calculations with good success. If a design similar to CDC is desired, then it could be done well using available data; however, if a new site or environment is desired, then calculational tools and analysis of the nuclear environment may be mandatory from the beginning.

ACID/BUTTERFLY MAIDEN

The stated objectives of the Airblast and Crater Induced Simulation Development (ACID) test assumed that it was the first test that addressed issues important in design and fielding a combined effects simulator in a dry alluvial material. In particular, three of the four basic test objectives were related to general CES effects and are: (1) Can a DIHEST provide the characteristics of a horizontal surface velocity waveform, or any other motion/stress parameter? (2) Can active instrumentation distinguish between HEST and DIHEST motions? (3) Can instrumentation be protected and ranged for both survivability and resolution? Even in the first CES series it was recognized that the nuclear criteria existed and must be met. Note that two of the three objectives of ACID concern the ability to measure the complicated and harsh environment. Only by accurately measuring the environment could it be determined that the criteria were met. ACID was supposed to be higher fidelity than a simple shake-rattle-and-roll test. However, defining the fidelity proved very difficult. The simulation was 1/4-scale of a 100-kt nuclear weapon at a range corresponding to 34 MPa, at that time considered to be a rather high pressure. Presently that is considered rather low, but the ground motions are difficult to simulate because of the long time separation of AI and DI ground shock.

Figure 3 shows plan and cross-section views of the test-bed. The HEST was designed to replicate the vertical motions and stresses for a period of 20 ms. This produced the proper peak vertical velocity up to a depth of 2.8 m. However, the arrival of the desired crater-related ground shock did not even begin until a time of 50-70 ms, clearly beyond the required vertical simulation time. The crater-related motions were to be simulated with the use of a standard DIHEST design (Ref. 10). The DIHEST was to yield the proper acceleration, velocity, and displacement.

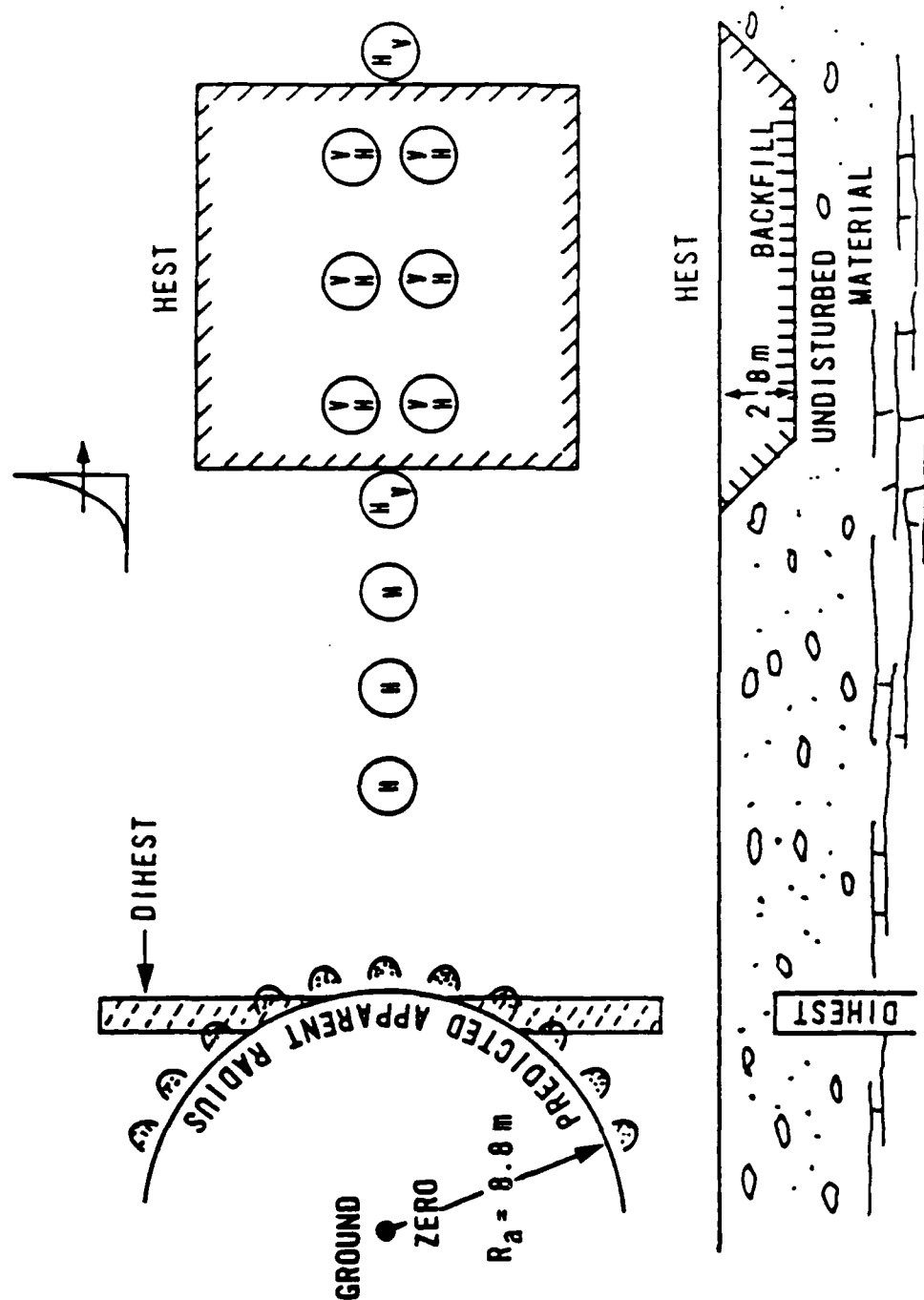


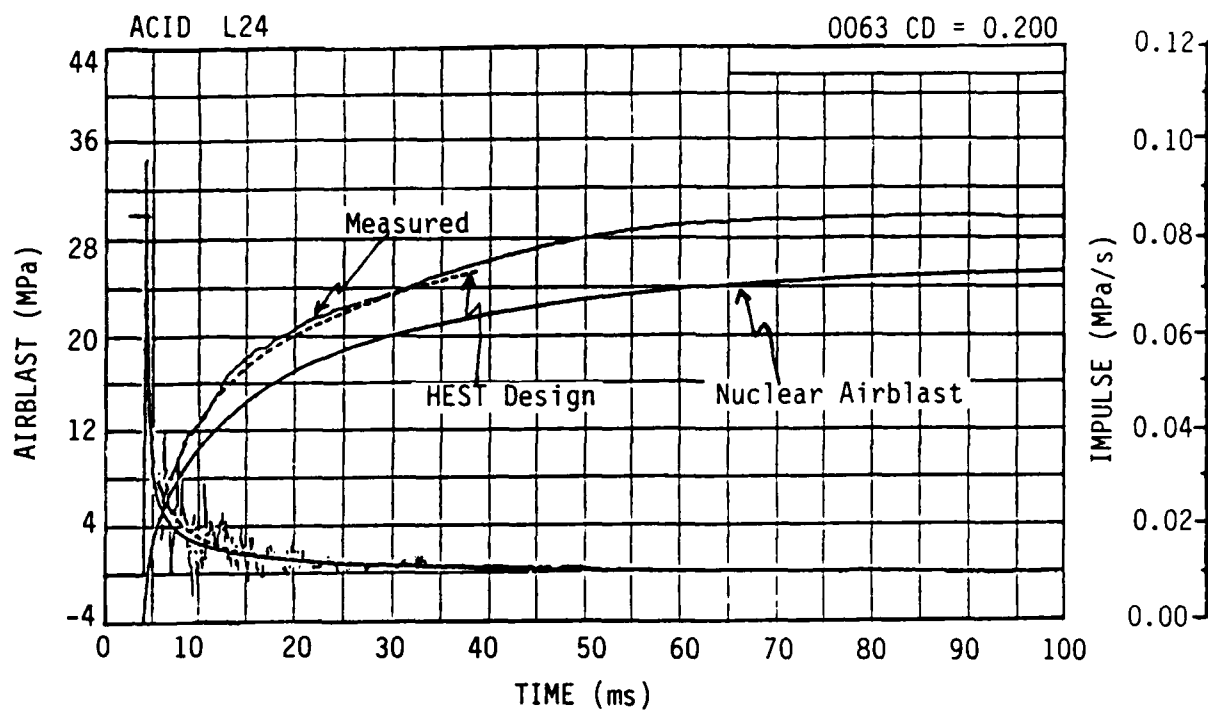
Figure 3. ACID test-bed with hand-calculated nuclear explosive crater.

As the DIHEST design developed, it was concluded that, to obtain all three motion parameters (acceleration, velocity, and displacement) correctly, the DIHEST would have to be placed at the predicted nuclear crater edge. In order to obtain the 50- to 70-ms time delay observed at the desired simulation area, simultaneous firing of the HEST and DIHEST was required (signals from the DIHEST had to travel a substantial distance before reaching the test article).

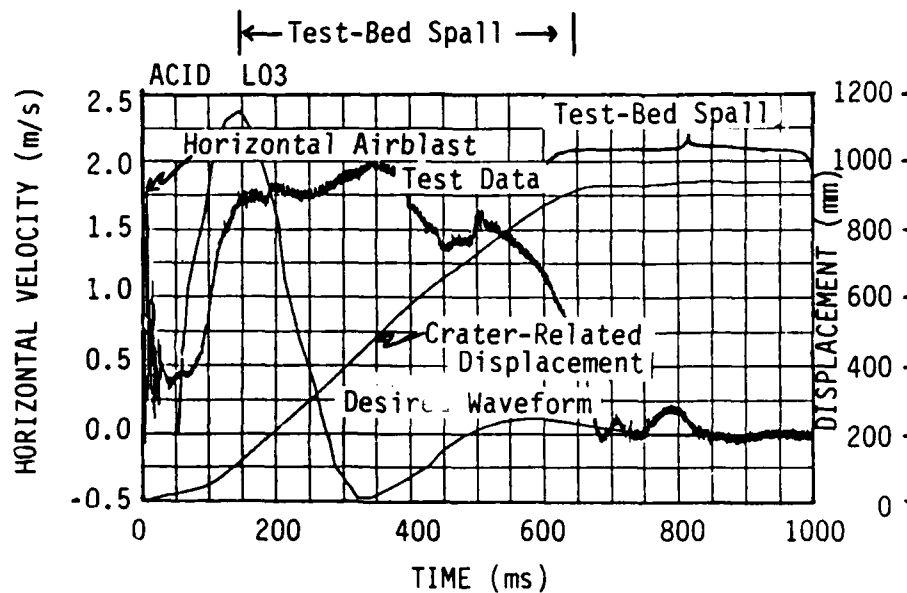
Figure 4 includes two data traces from the test. The upper one is the overpressure obtained from the HEST and the lower one a horizontal velocity trace from the simulation area. Also included in the horizontal record is the desired waveform, developed from the DIHEST prediction equations. The pressures and short-term vertical velocities were well simulated with the HEST using standard design techniques. The horizontal motions recorded from the DIHEST did not match the expected motions and included substantial increased displacement and very low stresses. It was concluded that the small size of the HEST created edge relief effects that left the test area in a state of spall (free fall and zero stress) during the time of crater-related motions.

This particular test contained four important lessons for designing a CES.

1. Since the first arrival is due to the airblast, design of the HEST can be done using the standard techniques.
2. The simulation times associated with a standard airblast-only HEST design (usually peak velocity or stress at some limited depth of interest) were insufficient to include the crater-related motion. The HEST was too small for long-term, total simulation (both velocity and stress histories).



(a) Vertical



(b) Horizontal

Figure 4. Pretest predictions and recorded waveforms for the CES ACID.
(Note different time scales.)

3. The HEST clearly affected the performance of the DIHEST motions and stresses. The DIHEST could not be evaluated using the standard design equations; simple superposition of simulators could not be done and the interaction of the HEST and DIHEST must be understood. In this case the HEST created a spall condition. As will be seen, the HEST initially creates compacted material through which the crater-related motions must travel if they are not to arrive during a spalled state. Or the CR motions must arrive during a compacted state if they follow the horizontal airblast very closely.
4. The early-time, horizontal velocity was measured. However, large baseline shifts created uncertainties in the later-time velocity-time histories. In this case, the late time was when the peak horizontal crater-related velocities were supposed to arrive. To obtain useful records, adjustments based upon passive displacement measurements were required.

ACID showed that some but not all necessary measurements could be made. Displacements from the DIHEST were factors of 2 too large because of the spalled test-bed. Following ACID, BUTTERFLY MAIDEN was fired. BUTTERFLY MAIDEN was a duplication of the ACID DIHEST but without the HEST. The BUTTERFLY MAIDEN HEST was fired a day or two after the DIHEST. BUTTERFLY MAIDEN correctly simulated the horizontal displacements.

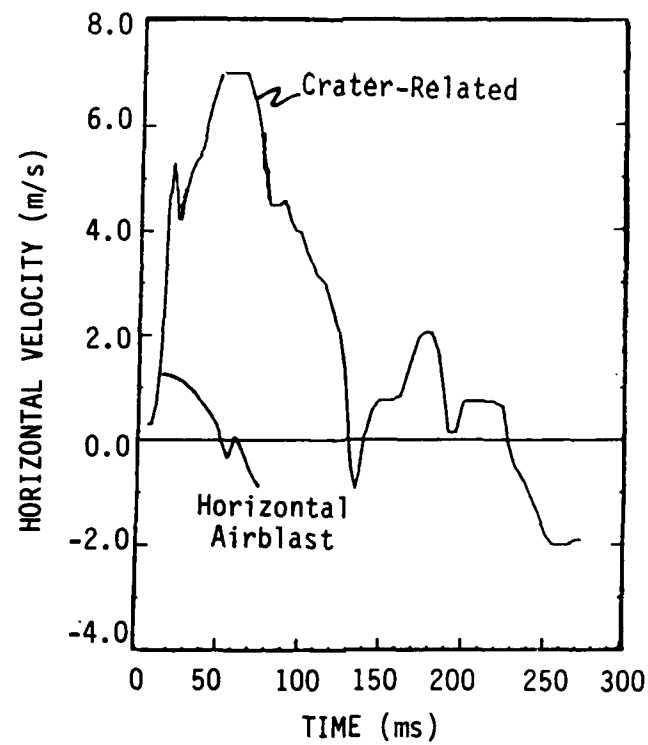
Although this particular simulator was of limited help in designing the higher overpressure CDC series, it did provide valuable information in understanding the physics of how two different ground shock simulators (a HEST and DIHEST) should be combined.

DESIGN PROCEDURE FOR A SPECIFIC CASE

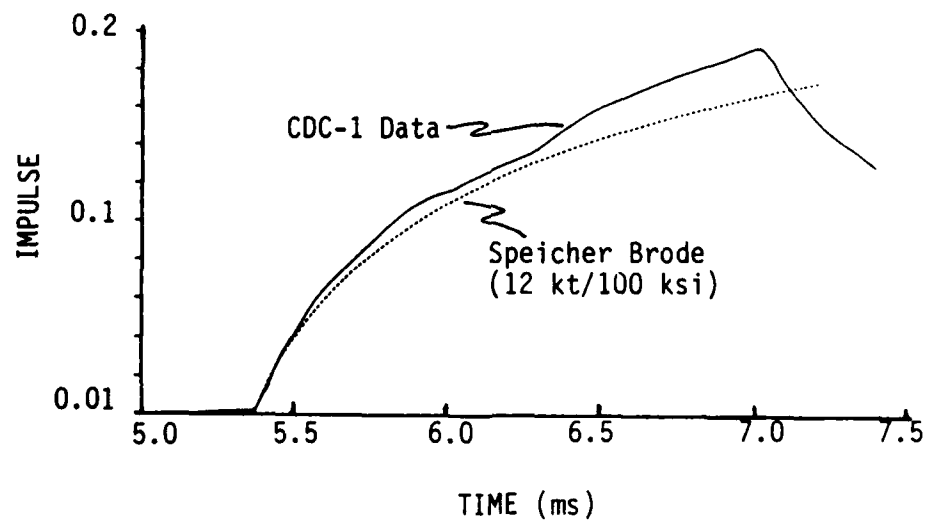
To understand the procedure for designing a CES, the example of CDC will be reviewed. The CDC series (Refs. 1 and 11) was a combination of experiments and calculations that developed a single combined effects simulator. This simulator produced the total velocity environment (both vertical and horizontal motions) of a large yield nuclear surface burst. It simulated a range of 700 MPa to 140 MPa (100 to 30 ksi) overpressures at full scale. Initial designs were calculated and fielded at yields of 2 kt, 12 kt and 96 kt. However, the full-scale test was canceled. The procedures used to design CDC not only give one an appreciation of how this series was designed, they also outline a method for designing other CESs. The final section of this report summarizes the design procedure for a full-scale CES at a dry site. However, several important details still need to be resolved. Instrumentation to measure the large displacements must be validated and an explosive charge must be designed to fire properly under the high hydrostatic loading in the deep DIHEST holes. Additional testing will be required to address those problems.

NUCLEAR ENVIRONMENT

Figure 5a shows the horizontal velocity waveform of the nuclear environment that was to be simulated. The waveform shown is for a depth of 3.8 m at a range corresponding to 80 ksi overpressure. Figure 5b shows the impulse to be applied by the airblast simulator along with data from CDC-1. This specification was simply the Brode-Speicher overpressure impulse at the appropriate range (in this case 100 ksi). Finally, Figure 5c shows the required time-of-arrival for the airblast simulator along with data from CDC-2.

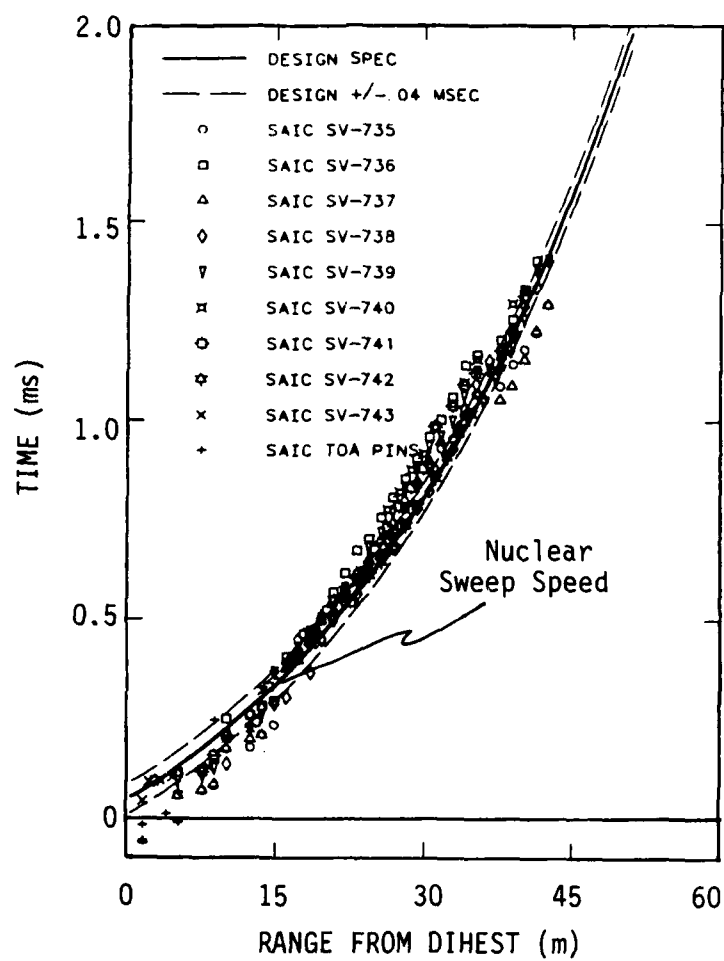


(a) Horizontal velocity histories.



(b) Impulse versus time.

Figure 5. Nuclear environment to which the CDC series was designed. (Only point examples are given.)



(c) CDC-2 arrival time summary.

Figure 5. Concluded.

From this environment, simulation criteria were developed for both the vertical airblast impulse and horizontal motions. These criteria took into account what was important in the simulation, the uncertainties of the estimates, and the ability to measure or validate that the simulator delivered the correct motions and stresses. The criteria for the vertical airblast specified a duration of 20 ms during which the simulator had to deliver an overpressure impulse-time history within 20% of the defined nuclear. The criteria for the horizontal ground shock were primarily in terms of motions and were related to modes of deformation (Ref. 12) of the free field. The modes were determined from a total motion field measurement over depths of interest for silo response. The criteria for the horizontal motion, given in Table 1, are in terms of rates and integrated rates of simple translation, tilting, and rotations about the center of mass of the simulation region. The modal analysis used to develop the criteria is similar to that used for structural response; however, no structure was considered. The measurements used for the analysis were from the free field.

There are several important aspects of the criteria. First, the total duration of the airblast simulation is much shorter than that required to meet the horizontal simulation (20 ms versus approximately 200 ms at 96 kt, although duration was not specified for the horizontal). This, in itself, implies that horizontal stresses associated with the CR wave, which are perturbed by the lateral edges of the HEST test-bed, were not important since the horizontal goal is predominantly motions, although CR stresses were to be less than the vertical airblast-induced stresses. Secondly, only horizontal peak rates (either translation, rotation, or bending) and totals (e.g., displacements) are given as criteria for the crater-related motions; that is, no specific histories were specified. Fortunately, in this material, this test series showed that if both the peak velocity and displacement criteria were met, then the waveform, or time histories, were adequate.

TABLE I
CDC-2 COMBINED EFFECTS FREE-FIELD
PERFORMANCE ASSESSMENT

	<u>Objective</u>	<u>Measured</u>	<u>Predicted</u>
Rigid Body Horizontal Motion			
Max velocity (V_m)	6.1 - 8.1 m/s	6.6 m/s	5.8 - 7.1 m/s
Max displacement (d_m)	0.23 - 0.9 m	0.6 m*	0.42 - 0.57 m
Risetime to V_m (t_r)	24 - 55 ms	40 ms	40 - 45 ms
Rigid Body Rotation			
Max angular velocity ($\dot{\theta}$)	0.33 - 0.44 rad/s	0.75 rad/s	0.82 rad/s
Max rotation angle (θ)	≤ 0.7 deg	≥ 1.5 deg	0.8 deg
Non-rigid Body Motion (Δ)	small	$\approx .001H$	$< .002H$

*Based on 5 records with durations greater than 150 ms.

An analysis of the nuclear environment was important in selecting the type of high-explosive arrays that should be used in the combined effects simulator. The vertical motions and stresses are dominated by the airblast; it arrives first. The initial horizontal velocity is the horizontal portion of the airblast. To produce the proper airblast-induced horizontal ground shock both the nuclear pressure gradient with range and time-of-arrival must be modeled (Fig. 5). This requires a variable HEST/BLEST. Since the airblast arrives first, standard HEST/BLEST design equations may be used without considering interaction with the DIHEST.

For this environment, the next important motion is the horizontal source-induced waveform of which only the crater-related (CR) pulse is apparent. The simulator that is generally used to produce the CR pulse is the DIHEST array. Reference 13 gives design equations for DIHEST simulators, but it does not account for any interaction with the HEST/BLEST. However, the nuclear environments calculation indicates that the CR wave arrives later than stresses from the peak vertical overpressure (Fig. 5). Thus, the CR motions are propagating through a soil already compacted by the airblast. All of the DIHEST prediction curves were obtained from material that was not compacted. There is no empirical data on which to base the design of the DIHEST when combined with the HEST. The environments also indicate a very small gradient of motions with respect to depth are apparent with the CR motions; this must also be modeled by the DIHEST simulator.

In summary, this specific nuclear environment may be simulated with the use of a HEST airblast simulator and a DIHEST simulator, although specific details of the DIHEST are not yet well known. Since the airblast arrives first, a design of the HEST will be straightforward using existing design equations. Some sort of DIHEST appears necessary to simulate the CR motions,

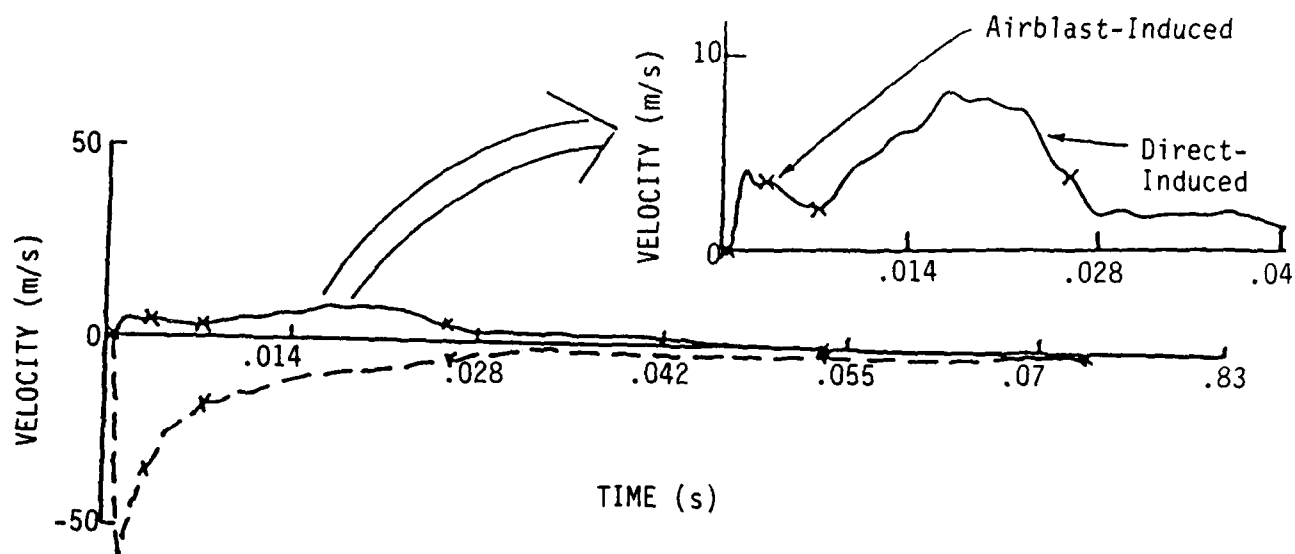
but there were few data on motions in material under compaction at the time of initial design. The additional criteria of small vertical gradients in the CR waveform adds further complication to the DIHEST design. Notice that it was the nuclear environment that dictated the selection of simulator components. If a different environment, e.g., different site, change in overpressure, different yield were specified, the CES may very well use more, less, or different types of explosive arrays.

INITIAL DESIGN

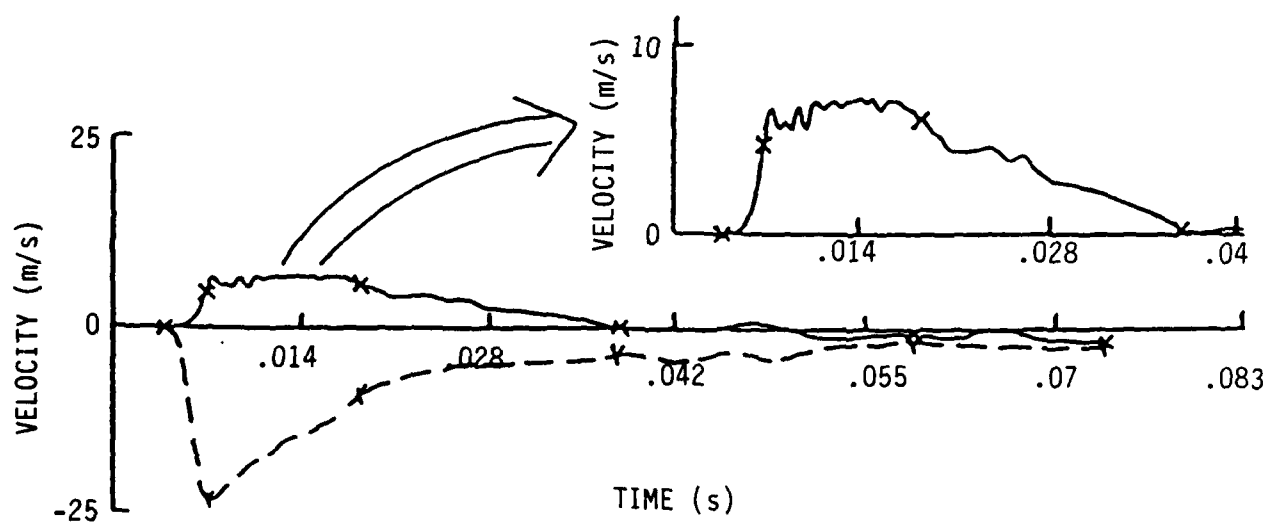
The analysis of the nuclear environment indicated that all of the motions could probably be simulated with the integration of a HEST and DIHEST. The specific criteria were not set until (1) the uncertainty of measurements was assessed, and (2) how well the calculationaly designed simulator would perform was determined. For this version final simulation criteria were set only for the last test, CDC-2. Figure 6 shows waveforms from a calculation of a nuclear surface burst. Such waveforms were used as the preliminary design criteria until specific criteria were adopted for CDC-2. Figure 6 shows the relative difference between the vertical and horizontal motions. The very high vertical accelerations generated by the airblast made measurement of the much smaller horizontal acceleration very difficult.

Figure 7 is a conceptual sketch of the planned simulator, with both its cross-section (Fig. 7a) and plan (Fig. 7b) views. In this figure, the solid lines indicate those portions that were well known--basically only the HEST charge parameters over the area of interest. The dashed lines refer to those areas where concepts were known, but details would have to be determined.

HEST. Initial estimates of explosive weights required for the HEST simulator could now be calculated using the relationships shown in Figure 8 (Ref. 3). These equations provide adequate



(a) Vertical (Y) and horizontal (X) velocities at 0.5-m depth.



(b) Vertical (Y) and horizontal (X) velocities at 3-m depth.

Figure 6. Horizontal and vertical particle velocity at the 13.9-m (75 ksi) range from the CRT 2-kt RM1 calculation (dry alluvium).

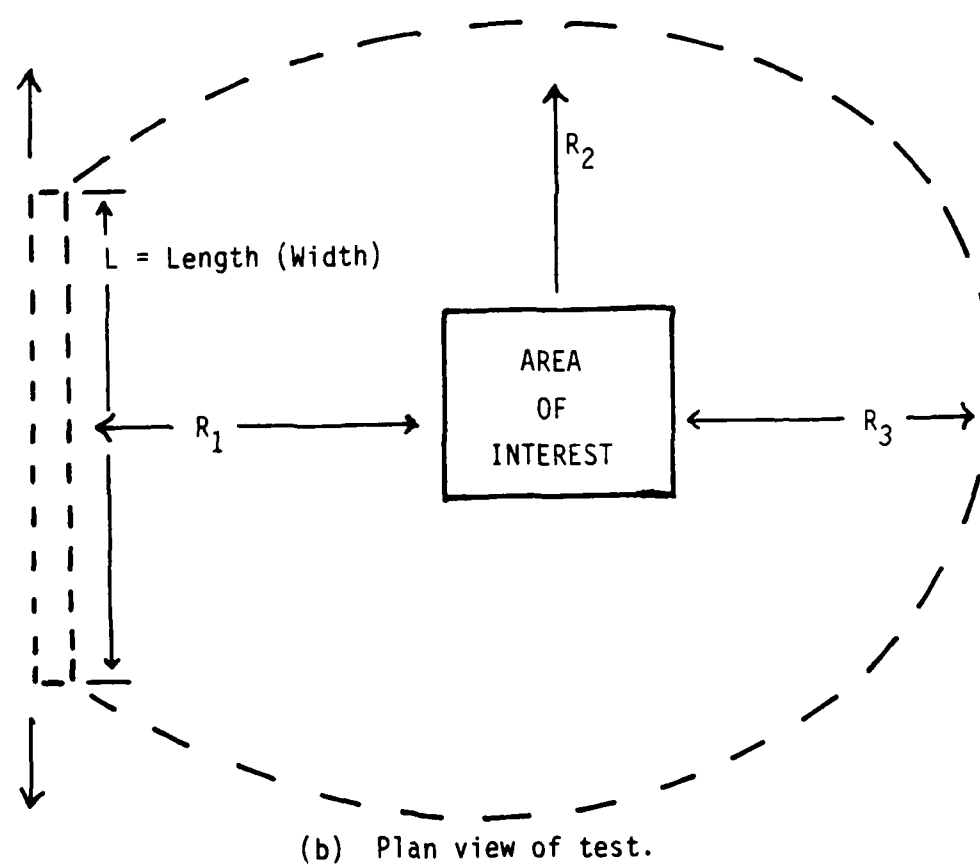
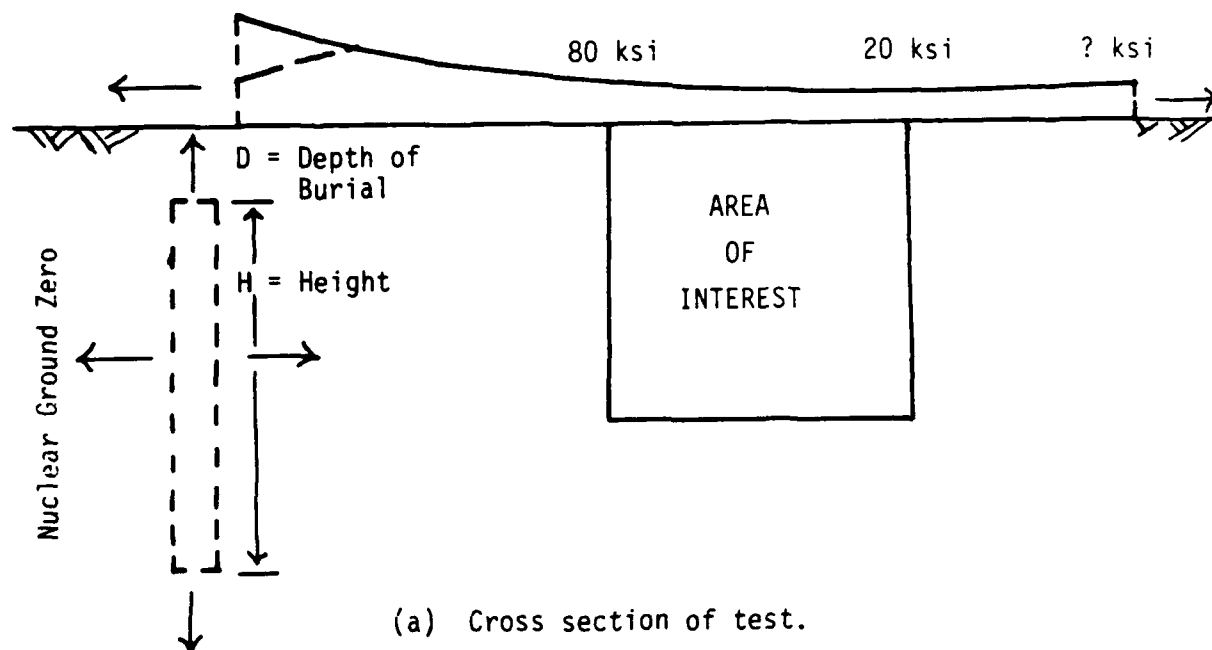


Figure 7. Generic conception of the CES simulator.

APPROXIMATE FORMULA FOR A VARIABLE HEST

Assumption:

- 1) YUMA Geology
- 2) Iremite 60 Explosive
- 3) TIGER JCZ-3 E.O.S.

$$\begin{aligned}
 h &= 2 Y^{1/3} \\
 H &= 2 Y^{1/3} \\
 m &= 1500 Y/R^2 \\
 w &= 21700 Y \log(R_2/R_1) \\
 h &= \text{Cavity Height (in.)} \\
 H &= \text{Overburden Height (ft)} \\
 m &= \text{Loading Density (kg/m}^2\text{)} \\
 w &= \text{Explosive Weight (kg)} \\
 &\quad \text{(Circular Test Bed)} \\
 Y &= \text{Yield (kt)} \\
 R_2 &= \text{Outer Radius of Test Bed (m)} \\
 R_1 &= \text{Inner Radius of Test Bed (m)} \\
 R &= \text{Nuclear Range (m)}
 \end{aligned}$$

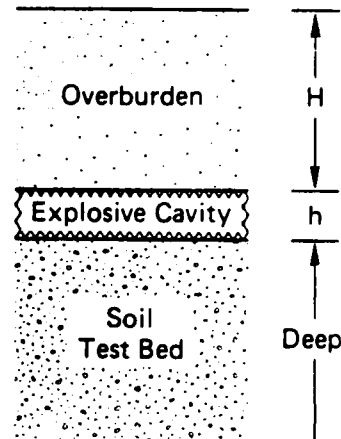


Figure 8. Initial design criteria for the HEST (after Ref. 3).

values for the start of a HEST design. Actual details of the design must be checked with 1-D calculations that include specific overburden densities and soil properties, details of explosive and foam placement, test bed preparation, etc. (Ref. 14). Tests show that the equations in Figure 8 give estimates that are within $\pm 10\%$ of actual values required. Notice that each pressure level requires different amounts of explosive and overburden. To obtain the pressure gradients required for the horizontal airblast, more designs for higher overpressures are required for upstream (from the test area) HEST parameters than for the test area or downstream. To implement this, the test bed is divided into finite areas (equated to dimensions of available materials, usually 4- x 8-ft sheets). The nominal range for each area is determined, and the design for that range is used in that area.

Figure 9 shows, as an example, the CDC-2 HEST test-bed design. The test-bed was first divided into panels 1.2 m by 2.4 m (2' x 4'), and the distance from nuclear ground zero to each panel was determined. A simple design, based on the equations given in Figure 8, was then calculated for each panel. For example, at a nuclear range of 50 m from a 96-kt weapon, panel 11 was calculated to have an explosive weight of 58 kg/m. Additional details of the design, for example the thickness of foam required to give the proper impulse-time history, were then calculated with computer codes. For future tests, an estimate of the required foam should be obtained from simple cubed root scaling of this design. Table 2 lists the specific values of the HEST panels for CDC-2 and could be used for generic designs of other HESTs.

The other major parameter needed to design the HEST is the size of the loaded area. The lateral extent of the HEST, R_1 , R_2 , and R_3 , (Fig. 7) controls the time of arrival of relief effects from the HEST edges. In dry soils these edge effects tend to

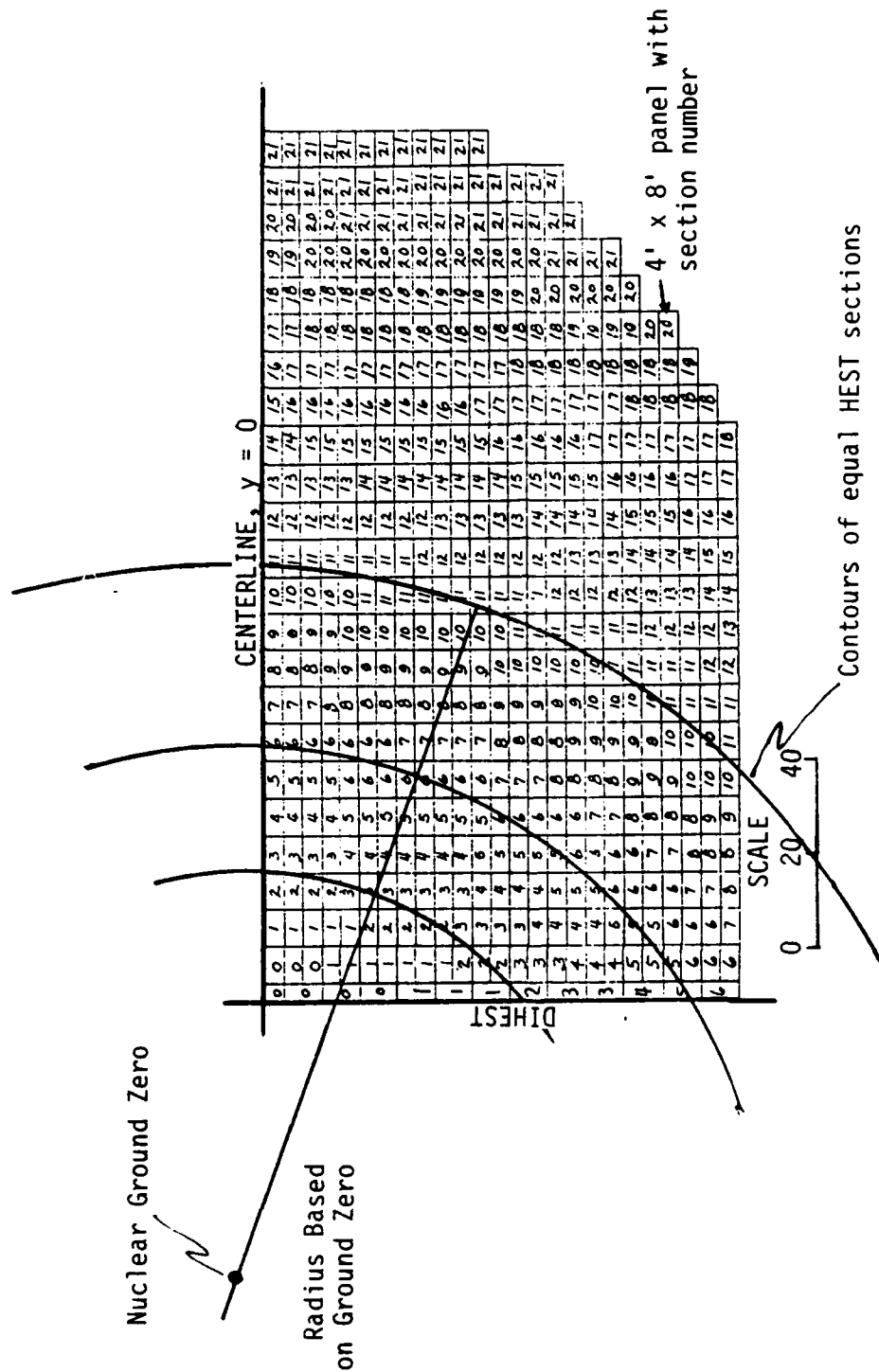


Figure 9. Plan view of simple HEST design for CDC-2, 96 kt, showing discrete 4- x 8-ft panels.

TABLE 2. CDC-2 PRELIMINARY HEST SIMULATOR DESIGN

Section Number	Iremite 60 Explosive Thickness ^a (cm)	Top Foam Thickness (cm)	Explosive Loading Density (kg/m ²)	Number of Panels Required ^b
0 ^c	3.543	None	262.5	13
1	2.783	None	206.15	30
2	2.434	0.323	180.34	26
3	2.129	0.626	157.735	40
4	1.864	0.894	138.105	46
5	1.635	1.122	121.1	56
6	1.439	1.319	106.575	70
7	1.269	1.488	94.005	36
8	1.124	1.630	83.3	56
9	1.002	1.756	74.2	56
10	0.897	1.858	66.475	58
11	0.809	1.945	59.965	70
12	0.735	2.020	54.455	56
13	0.672	2.082	49.785	34
14	0.619	2.138	45.82	42
15	0.572	2.185	42.41	42
16	0.533	2.224	39.465	46
17	0.497	2.260	36.84	64
18	0.465	2.291	34.475	74
19	0.436	2.319	32.315	26
20	0.409	2.346	30.301	50
21	0.383	2.374	28.395	90

1081

^a Cast Iremite 60 explosive based on 1.12 g/cm³ solid density.

^b Based on Figure 9, times 2.

^c Section 0 has no bottom (2-in-thick) foam.

reduce peak velocities and peak stresses. Estimates of R_2 and R_3 are determined from the shear and unloading velocities of the site and the simulation times.

$$R_i = t_{sim}/(C_S \text{ or } C_U); i = 2 \text{ or } 3 \quad (1)$$

where t_{sim} is the desired simulation time of the HEST and C is the appropriate velocity--unloading wave velocity for peak stresses and S-wave velocity for peak velocities (Ref. 15). Experiments have shown that the full impulse need not be used at the lateral extents of the HEST to attain the appropriate loading within the area of interest--when only a single airblast loading is required. At the high pressure edge, the later time pressures arrive at the area of interest too late with respect to the simulation time and could, perhaps, be neglected. But, for this particular type of simulator, the full impulse is required in order to limit the crater created by the DIHEST to a size that will not intersect the area of interest. Determination of the amount of explosive reduction at the other edges of the HEST requires ray tracing techniques beyond the scope of this report, but they are possible.

DIHEST. The design of the DIHEST and integration with the HEST airblast simulator was the major unknown in this test series. As indicated with the dashed lines and arrows in Figure 7, none of the DIHEST parameters were predetermined. The entire explosive charge had to be designed from scratch.

As a starting point, equations from Drake (Ref. 13) were used to predict the output of a simple DIHEST. These equations do not account for any HEST/DIHEST interaction and come from limited test data. For these reasons Drake's equations were used only as a starting guide. Reference 13 considered all of the DIHEST data and was able to collapse it into a prediction scheme that relied upon knowing the length of the DIHEST (L), the height

of the DIHEST (H), the areal density of the charge (α) and the range away from the charge array. The results, giving predicted peak accelerations, velocities, and displacements are (Dry Soil)

$$\begin{array}{lll}
 & 760 (\alpha/R)^{5/3} & R < H/2 \\
 a\alpha = & 760 (\alpha/R)^{5/3} (H/2R)^{2/3} & H/2 < R < L/2 \quad (2) \\
 & 760 (\alpha/R)^{5/3} (H/2R)^{2/3} (L/2R)^{2/3} & L/2 < R
 \end{array}$$

$$\begin{array}{lll}
 & 5.9 (\alpha/R)^{2/3} & R < H/2 \\
 v = & 5.9 (\alpha/R)^{2/3} (H/2R)^{2/3} & H/2 < R < L/2 \quad (3) \\
 & 5.9 (\alpha/R)^{2/3} (H/2R)^{2/3} (L/2R)^{2/3} & L/2 < R
 \end{array}$$

$$\begin{array}{lll}
 & 0.038 & R < H/2 \\
 d/\alpha = & 0.038 (H/2R) & H/2 < R < L/2 \quad (4) \\
 & 0.038 (H/2R) (L/2R) & L/2 < R
 \end{array}$$

where α is the areal charge density in kg/m^2 , a is the acceleration in g 's, v is the horizontal velocity in m/s , d is the displacement in m , and R is the range from the center of the DIHEST.

Although the number of tests that make up this data set is rather large, it is limited in material types, areal densities, and charge geometry. The length-to-height ratios of the tests were usually 3 to 1. Depth of burial of the top of the DIHEST was usually one-half of the charge height. The areal charge densities were usually less than 50 kg/m^2 . Almost all of the tests were fired at McCormick Ranch in dry alluvium. There are essentially no data in the range of $R < H/2$; however, this is the data base and should be used in very preliminary scoping of the problem.

Referring to Figure 7, Equations 2, 3, and 4 can be used to estimate the range from the area of interest (R_1), height (H), and length (L) of the DIHEST needed to meet the simulation criteria. The initial criterion for the CDC series was a peak horizontal velocity of 10 m/s.

Figure 10 shows what Drake's prediction looks like for a given DIHEST design and how varying design parameters will change the simulator output. Figure 10a shows the predicted peak velocity for a given DIHEST design. (Peak acceleration and peak displacement would be similar.) Note that the prediction is divided into three regions--planar, cylindrical, and spherical. The planar, or 1-D, region is that region so close to the charge that the edges of the charge are relatively far away. In this region the charge is essentially infinite in area and the attenuation of peak velocity is due only to hysteresis in the material (frictional losses and crush-up of the soil). The next region is the cylindrical or 2-D region. This region is far enough away from the charge that the height of the charge (the shorter dimension) is relatively small but the length is still relatively large. In this region the charge is essentially a horizontal cylinder infinite in length but finite in diameter. The attenuation of peak velocity in the cylindrical region is caused not only by the hysteresis of the material but also by the expansion of the wave in the cylindrical geometry. Another way of describing the increased attenuation in the cylindrical region is to say that two of the four sides of the charge are now close enough that they perturb the originally planar wave. This perturbation causes an increased attenuation. In the spherical or 3-D region both dimensions of the planar charge are relatively small. The wave is now expanding in a spherical geometry and the attenuation increases. Put another way, the initially planar wave is now perturbed by all four sides of the finite charge and the attenuation is greater than that in the cylindrical region.

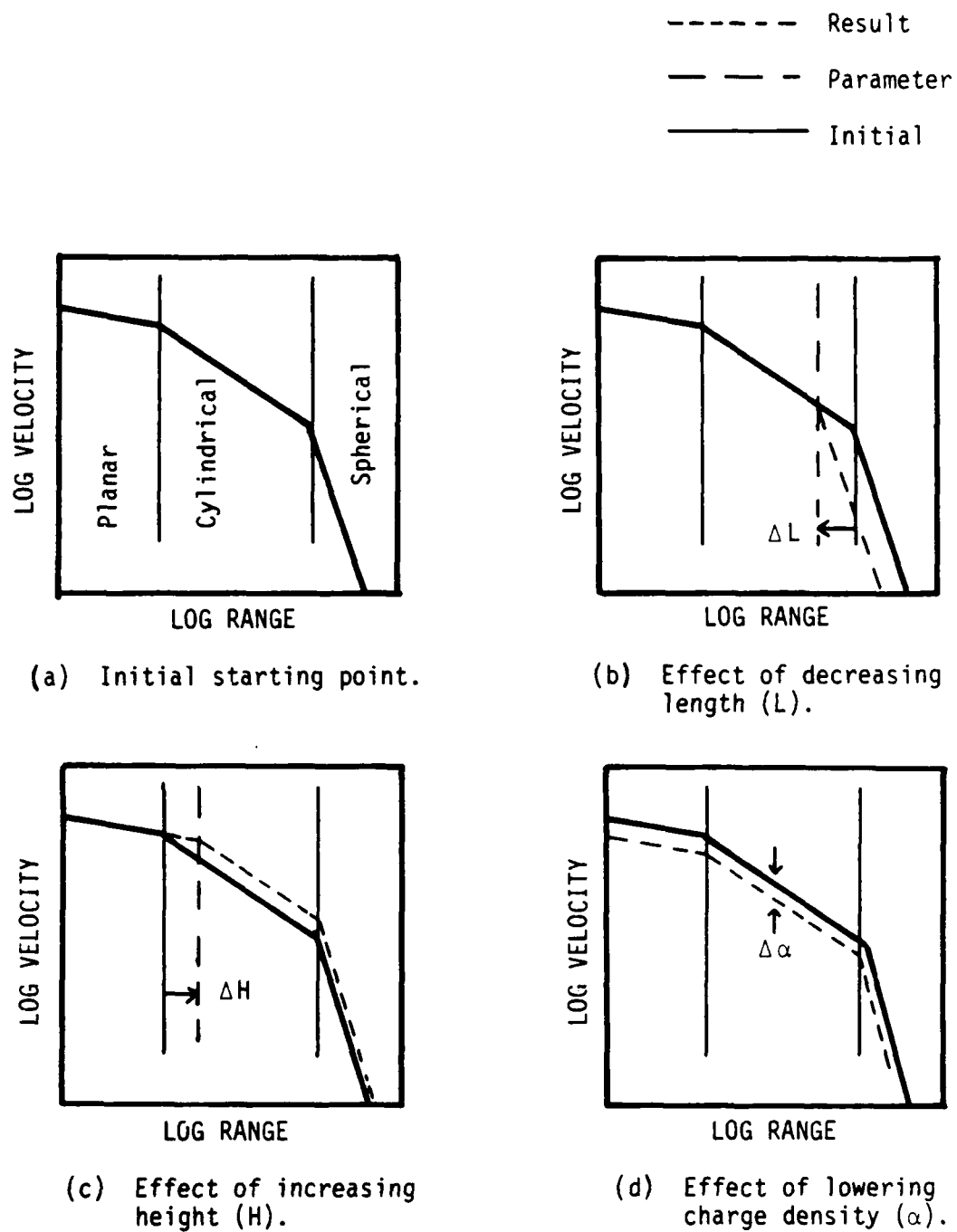


Figure 10. Effects of changing parameters in DIHEST design.

The output of the DIHEST can be changed by changing the length (L), the height (H), or the areal loading density (α). Figure 10b shows the effect of increasing L. Figure 10c shows the effect of decreasing H. Figure 10d shows the effect of increasing α .

For the CDC series, the choice was made to keep L/H approximately equal to 3 or 4 (3 for CDC-1 and 4 for CDC-2) because of the available data set and the observation in Pre-CARES that for smaller ratios the lateral area of interest would be substantially reduced because of the outward flow caused by the edge effects. Certainly other choices, especially going to wider and/or longer simulators, could be considered; however, resources limited the number of parametric studies which could be accomplished.

Pre-CARES (Ref. 17) data also indicated that the width of the DIHEST should be approximately twice the distance to the test article. In other words, referring to Figure 10, the test article should be placed near the transition from cylindrical to spherical regions of the DIHEST, probably more on the cylindrical side.

The next parameter to consider is the range, R, that the HEST is away from the DIHEST. Clearly, the amplitude of the velocity (and the other parameters) are affected by the range; and, if only a DIHEST were to be fielded, then a solution to Equations 2, 3, and 4 could be obtained for the optimum range (and areal densities). However, consideration must be given to the placement of the DIHEST with respect to the HEST. The ACID results indicated that if the separation is too great, deleterious effects could result. On the other hand, if the DIHEST were placed under the HEST, then the DIHEST would be physically affected by the detonating HEST creating perhaps a lower confidence in firing of the DIHEST. Therefore, for

simplicity, firing surety, survival, ease, etc., the DIHEST was positioned at the edge of the HEST; the edge being established by the required airblast simulation time.

Finally, the height of the DIHEST had to be chosen. In order to prevent a large vertical gradient in the horizontal motion produced, the height was chosen to be approximately equal to the height of the target that would be tested.

Note that the parameters chosen for the final DIHEST design led to a DIHEST-only simulator that would lead to cratering of the area of interest and particle velocities that are almost double those required. The HEST limited the cratering and, as it turned out, the velocities. Calculations indicated that this would happen, but again there were no empirical data.

Now the general dimensions of the DIHEST were known. Range was chosen to be at the edge of the HEST. The length was chosen to be greater than twice the range, (to keep the target in the cylindrical region). The height was chosen to be approximately equal to the target height. This left the charge density and depth of burial to be determined. Parametric calculations were used to adjust these two parameters.

Figure 11 compares calculations and data from Pre-CARES. It shows how the DIHEST motions were affected by the HEST. Basically, the material is precompacted by the HEST; and, at the area of interest, the horizontal velocity is reduced by interaction with the HEST. Details of the interaction are given in the next section. It is important to understand that calculations were needed to determine how the HEST affected the DIHEST motions and thereby determine the areal charge density needed in the DIHEST.

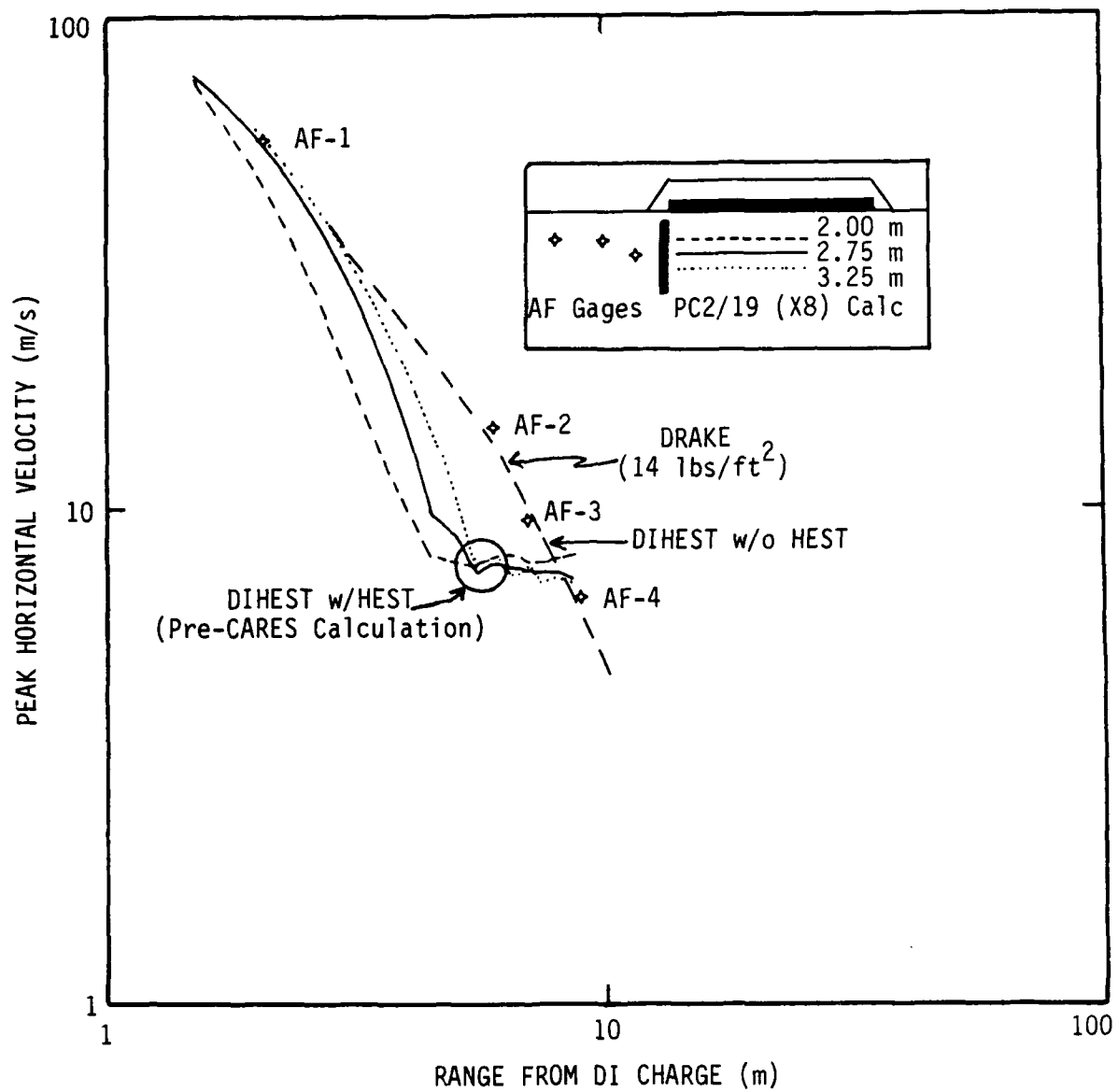


Figure 11. Effect of HEST on DIHEST free-field motions for Pre-CARES.

Figure 12 (again results from calculations) shows the effect of the depth of DIHEST from the surface. The original criteria required "small" vertical gradients of the horizontal velocities. As can be seen from this figure, the gradients were reduced as the depth of burial of the DIHEST was reduced. Thus, the CDC series was designed with the DIHEST as close to the surface as possible.

Figure 13 is a cross-section view of the CDC-2 simulator as fielded. In summary, with more details in the following section, the DIHEST design was made with:

1. Range (R_1) determined by location of HEST for airblast simulation times. The DIHEST was placed at the leading edge.
2. The width (L) was such that the test article was within the cylindrical region of the DIHEST.
3. The depth beneath the surface, based on calculations, was small for little vertical gradients of horizontal velocity.
4. The height of the DIHEST (H) was limited to $1/4 L < H < 1/3 L$ and chosen such that the bottom of the test article was at the centerline of the DIHEST.
5. The charge density was established through calculations, with Drake's free-field estimates being used as a starting point only.

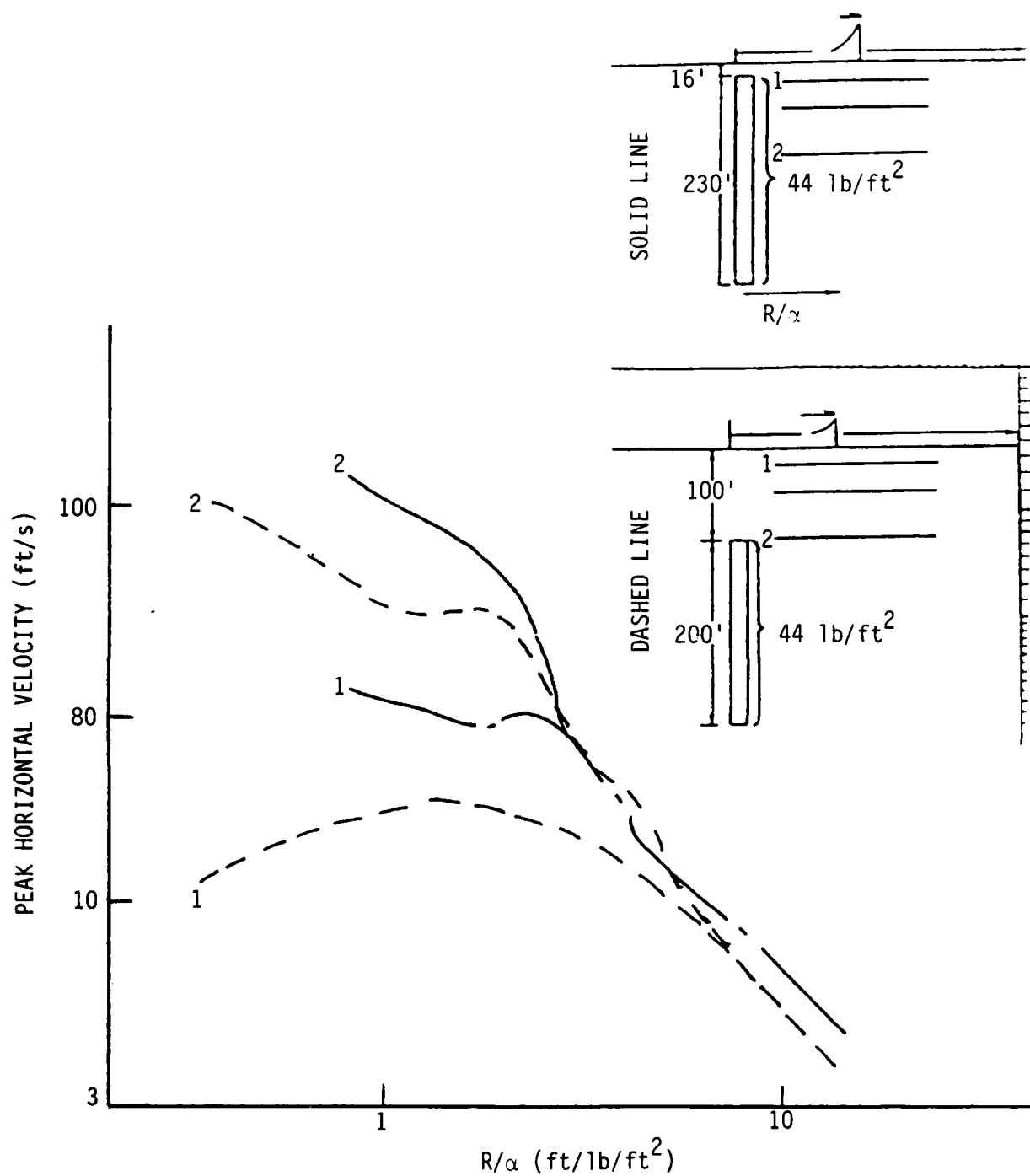


Figure 12. Effect of depth of burial of DIHEST on vertical velocity gradient.

0 10 (m)
Scale

HST (see Fig. 9)

3 m →

DIHST

Explosive Type	ANFO
Length of DIHST	61.2 m
Depth of Charge Top	3.0 m
Height of Charge	13.4 m ²
DIHST Area	820 m ²
Total DIHST Weight	91800 kg
Areal Density	112 kg/m ²

Figure 13. Cross section of CDC-2.

DESIGN PROCEDURES FOR CES IN DRY SOIL

GENERAL

As we have discussed, the limited number of experimental data sets of combined effects simulators does not allow presentation of a general empirical design procedure for a general simulator. The procedure followed for development of the fielded simulators was to combine simulator types. Individually, these simulators were understood, but the results of combining them could be determined only through calculations. Especially important were the modifications to the source-induced motions from the DIHEST. Thus, at present, designs for CES require extensive calculations if any assurance is to be placed in their outputs.

Figure 14 is a profile view of a generic CES showing the area divided into two regions of first arrivals. Directly beneath the HEST, the first arrival is from the airblast simulator and the theory associated with this design is well understood. Note that this region includes the "area of interest." Beneath a line beginning at the intersection of the DIHEST and HEST, assuming simultaneous firing of the two simulators and extending downward at an approximate 45-deg angle with respect to the surface, the initial arrivals are the motions from the DIHEST. The transition boundary will change as the position of the DIHEST and firing times change from case to case, but, in general, the transition can be located from simple theory. For example, one of the cases given delays firing of the DIHEST until stresses from the HEST completely envelop the DIHEST (hard to field but easy to calculate). In this case, all initial motions will be due to the HEST and there would be no transition region. The motions from the DIHEST would always be in perturbed material. First arrivals, and their associated stresses and motions, can be calculated from existing procedures developed for

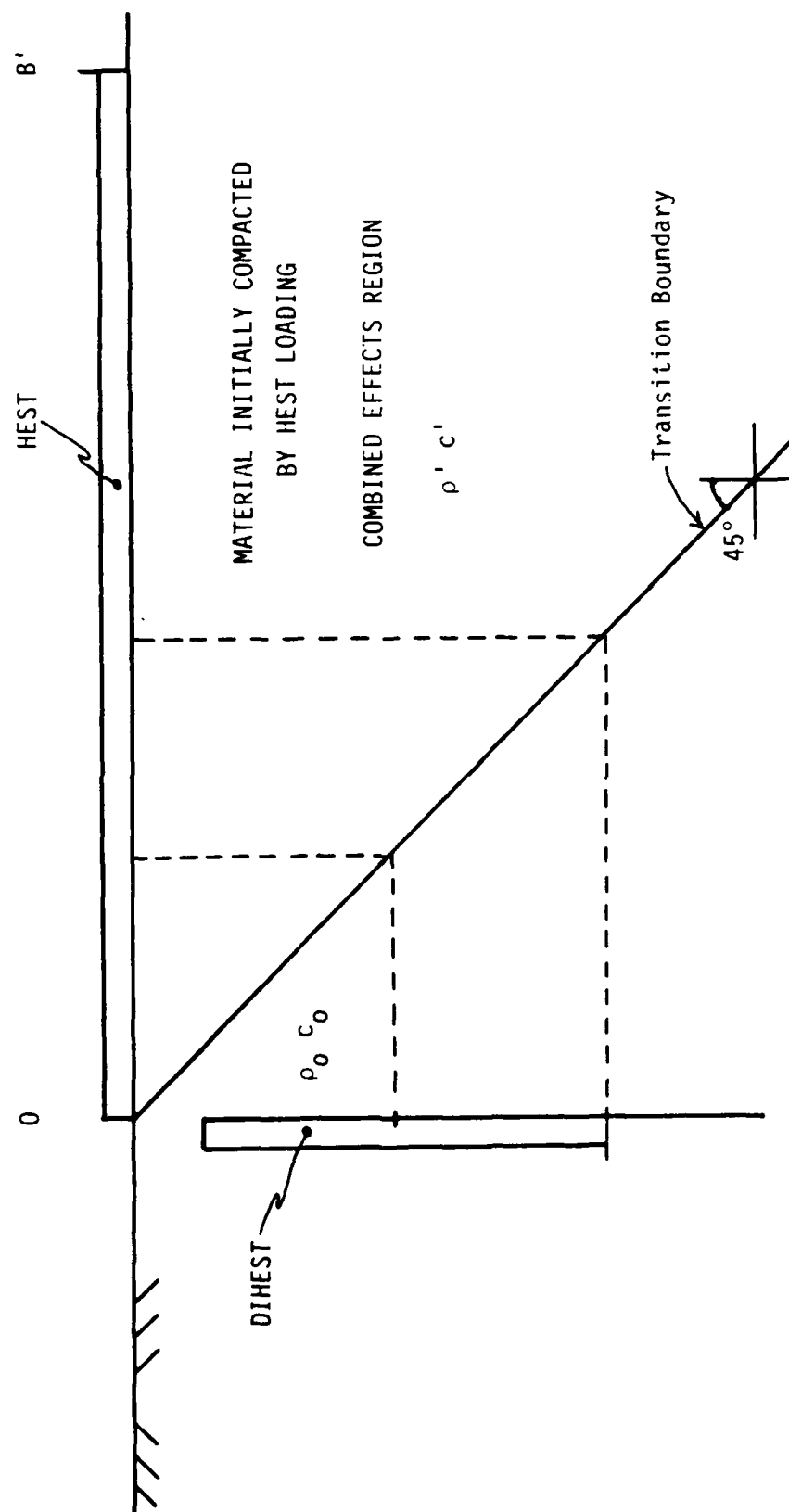


Figure 14. Profile view of combined effects simulator test-bed.

the appropriate single simulator. In Figure 14, the DIHEST Equations 2, 3, and 4 would be correct below the transition zone.

The second arrivals, HEST motions below the transition boundary and DIHEST motions above, are then a direct result of reloading and unloading material properties. Dry materials are highly nonlinear and hysteretic so that second arrivals cannot be a simple superposition of the two simulators. On the other hand, saturated, wet materials are more elastic so that second arrivals could very well be a simple superposition of the two simulators. This section will deal primarily with dry, hysteretic materials with extension of the methodologies being presented in a later section.

The changed properties seen by the secondary arrivals are indicated by the primed variables (ρ' , c'). Since initial crushing out of the air will tend to increase both the density and wave velocities, particle velocities of the second arrivals should be less than if they are first arrivals. If the situation were one-dimensional, simple application of impedance differences could be used to estimate the new velocities and stresses; however, the three-dimensional aspect requires calculational or empirical fits to the data.

This section presents calculations that were run in establishing the particular parameters, presented in the last section, for CDC-2. The calculations are quite specific and yield specific results, but they are insufficient for providing other than a qualitative understanding of the parameters for a general design. They could be used as an aid in extrapolating the CDC results for different scales and other, limited overpressures (e.g., extension from 700 to 100 MPa).

Following the calculational series, data from CDC-1 will be discussed. The data show explicitly the effects of

precompaction. From the calculations and data, a general procedure will then be developed.

CALCULATIONAL MODELING

Calculationally, an infinite extent HEST is easily represented in one-dimensional geometry. The details of charge build up, explosive, foam, berm, soil, cavities, etc. can be modeled in any desired detail, or, more simply, a Brode-Speicher airblast function could be used. As finite boundaries are added, two-dimensional calculations can be made to replicate, adequately, most of the phenomenology. For example, Reference 16 has shown that square HEST, with four edges can be modeled satisfactorily using axisymmetric geometry.

On the other hand, even a simple free DIHEST problem is fundamentally three-dimensional as illustrated by Figure 15. The three-dimensionality of the problem is even more apparent when the HEST is added. Although three-dimensional codes are available, limitations imposed because of their size and resolution of fine details precludes their use as a design tool. Thus, assumptions and simplifications must be made to allow the use of the two-dimensional codes. The two most basic simplifications concern the modeling of the individual charge holes used in DIHEST construction, and the arrival of edge effects from the DIHEST's boundaries.

As opposed to the HEST, which can be modeled as a simple pressure boundary, motions and stresses from the DIHEST are a result from both the initial boundary conditions, but also are a result of how the cavity created by the explosives grows and collapses. Thus, modeling of the DIHEST should be accomplished with the use of explosive burning and cavity expansion. In the field, DIHESTs are usually placed with a series of cylindrical, discrete drilled holes filled with explosive. A continuous slab

of explosives is seldom used because of the difficulty of constructing such a charge. However, the 2-D calculation cannot model the individual borehole charges. Instead the DIHEST is modeled as a continuous slab. The areal charge density (α) of the DIHEST is

$$\alpha(\text{DIHEST}) = \frac{(\# \text{ holes})(\rho_{\text{explosive}})(\text{hole volume})}{HW} \quad (5)$$

where

$\alpha(\text{DIHEST})$ is the fielded areal density

$\rho_{\text{explosive}}$ is the density of the explosive

H = height of hole

W = distance between the outermost hole centerlines

This areal density could be related to a solid filled trench with appropriate thickness; however, energy loss results from the expansion of individual DIHEST cylindrical holes to make a single cavity. Thus, an efficiency factor must also be included for the proper areal density used in the calculations. The areal density used in the calculations modeling boreholes with a slab is then

$$\alpha(\text{calculation}) = \alpha(\text{DIHEST}) (\text{E.F.}) \quad (6)$$

E.F. is the efficiency factor (≈ 0.65).

The $\alpha(\text{calculation})$ is lower than the $\alpha(\text{DIHEST})$. The value of E.F. was estimated from a combination of calculations and experimental data (CDC-1). The calculations considered a plane normal to the cylindrical drill holes and compared particle velocities with those calculated from a simple slab charge. A value of 0.65 (Ref. 17) was obtained. This value appeared a bit low in comparison to CDC-1 data, but the data were not conclusive. However, a value of 0.85 proved correct for CDC-2.

The second effect that is not calculated with the 2-D calculational geometry is the edge relief effects coming from the lateral (as opposed to the bottom) edges of the DIHEST. These edges would tend to reduce the peak horizontal particle velocities at ranges of approximately W/Z . No sound method, other than a 3-D calculation, would be able to properly account for these edges. However, the area of interest was placed in an area of cylindrical divergence so the lateral edges would not affect the peaks. Thus, it was reasoned that motions and stresses calculated for the area of interest and closer to the DIHEST would be representative up to the time of peak horizontal velocity and for some time thereafter. For regions beyond this, the calculations would be an upper bound. Experiments were planned to obtain empirical data to account for this, but the data were inconclusive.

In summary, the calculational setup was as seen in the right portion of Figure 15b. The HEST was modeled as a pressure boundary using the Brode-Speicher airblast function. The DIHEST was modeled as slab explosive (with the JWL equation-of-state, Ref. 18) with an efficiency factor included. The parametric studies investigated geometric placement, size effects, and the timing of firing.

CALCULATIONAL SERIES

The calculational series can be broken down into three basic efforts. First, as a starting point to understand better the effects of the HEST on the DIHEST, a short series of DIHEST-only calculations are presented (from Ref. 19). Following that, two short parametric series, one by NMERI (Ref. 20) and one by CRT are discussed. From the series, a good qualitative understanding of the important parameters will be gained.

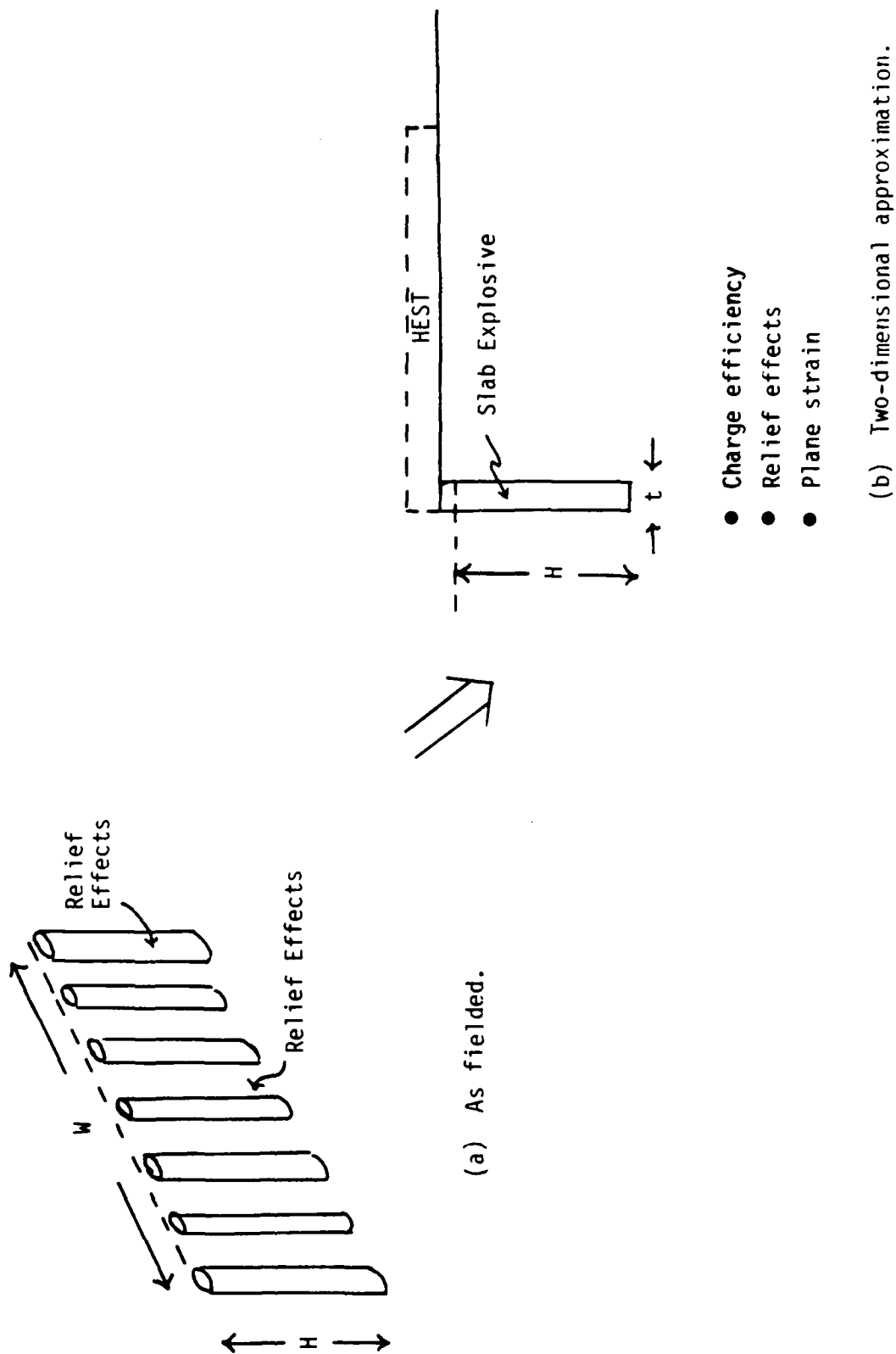


Figure 15. Modeling of the DIHEST for the calculations.

DIHEST

Figure 16 shows the results, in horizontal velocity, of three DIHEST-only calculations (Ref. 20). Parameters important to the 2-D calculations are shown in the lower portion of the figure. These calculations were done by NMERI and a word concerning the particular ranges, depths, etc., is important. All of the calculations done by NMERI (these and the ones for the CES) are based or scaled to the dimensions of a 225-kt nuclear surface burst with the point of interest at a range of 67.9 m from ground zero. All ranges are given with respect to the true nuclear; that is, a range of zero corresponds to nuclear ground zero and a range of 67.9 m corresponds to a nuclear overpressure of 500 MPa (70 ksi). Most point comparisons are associated with a target range of 67.9 m and a desired peak horizontal velocity of 10 m/s. As some basis, the results for the 2-D DIHEST only calculations are shown in Figure 16. Equations 2, 3, and 4 suggested that either a DIHEST with an areal density of 36.6 kg/m^2 (calculations 2a and 2b) or an areal density of 121.4 kg/m^2 (calculation 2c) could provide a horizontal velocity of 10 m/s at a nuclear range of 67.9 m. Note that the DIHESTs are located in different locations. The calculations show that for points along the DIHEST centerline (depth = 6.1 m), this velocity was achieved, and these estimates serve as a basis from which to understand the effects of the HEST.

Calculational results for the DIHEST-only series are also shown for two other depths (1.5 and 9.1 m). Note that for all cases the near-surface velocity is reduced because of the free-surface effects. Although not shown until later, the near-surface horizontal stresses are quite low, again because of the free surface. The difference between 6.1 m and 9.1 m is not substantial until the DIHEST is moved upward (calculation 2b). Then 9.1 m is below the explosive charge and the velocity is reduced. Although the calculations were only run to 50 ms,

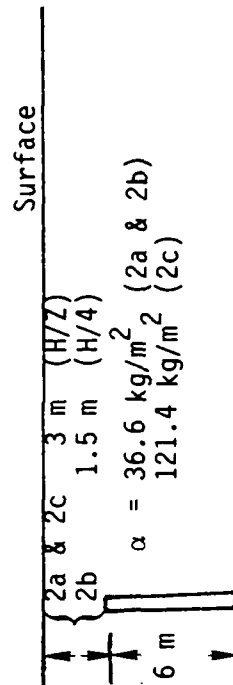
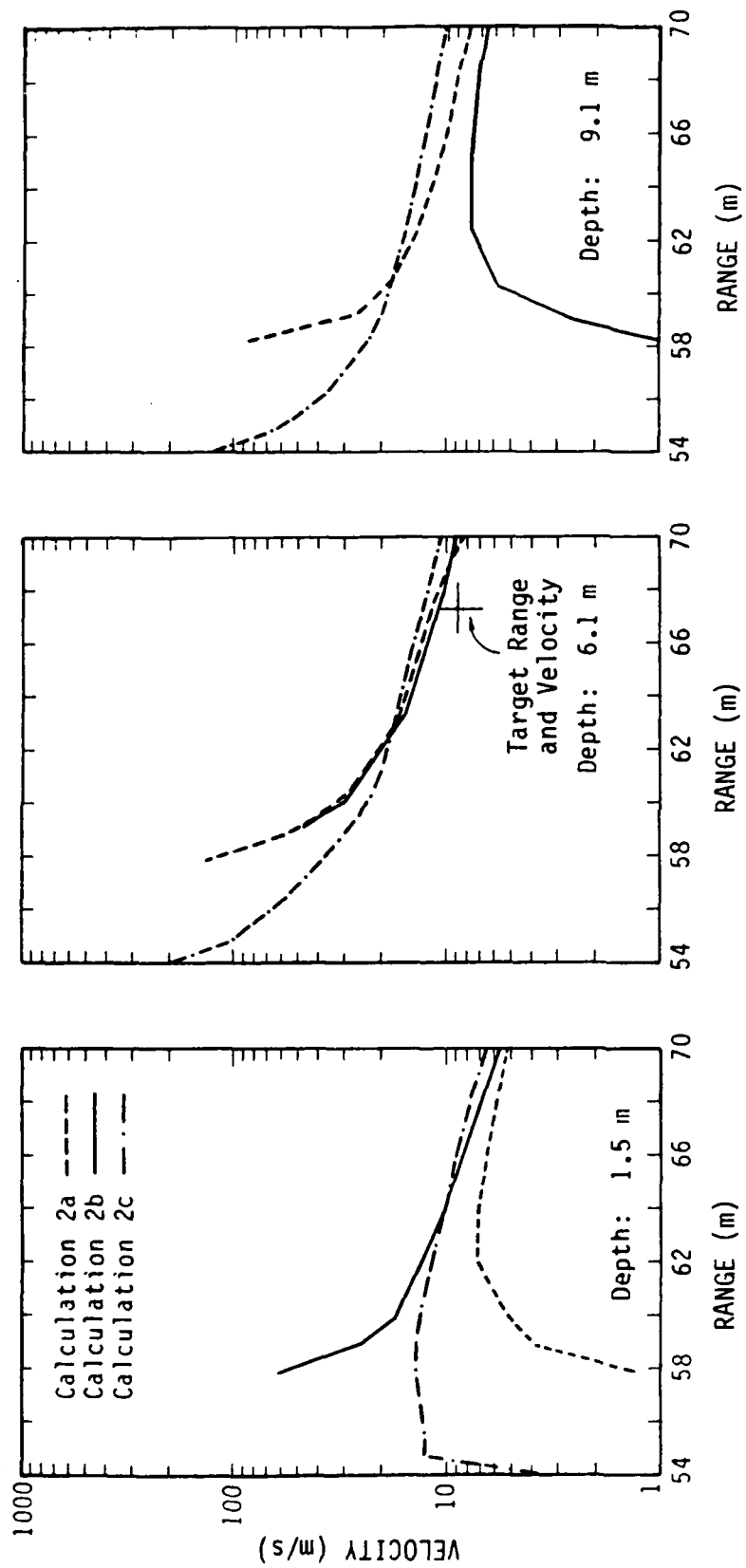


Figure 16. Peak horizontal velocity versus range for DIHST only.

empirical estimates, both from DIHEST-only experiments and the CDC NMERI calculational series, show that the crater would intersect the target points.

With this as a basis, a Brode-Speicher overpressure function was added to represent the HEST. Peak overpressures used in the calculation are shown in Figure 17. Again, these values are for a 225-kt surface burst with the range given as true nuclear. The airblast function was zero for areas not covered by the HEST, and used the values of Figure 17 where it existed. Figure 18 depicts the six parametric calculations done by NMERI. The dimensions are accurate in this figure and indicate the areal location of the HEST with respect to the nuclear (Fig. 17), and the true location of the DIHEST with respect to the HEST. In all cases except 4, the HEST and DIHEST were "fired" simultaneously; the DIHEST in 4 was "fired" as the peak velocity from the HEST reached the bottom of the DIHEST. Simple transition lines separating HEST or DIHEST first arrivals are sketched in. Also indicated are the areal densities of the DIHEST (α).

To see the effects of the HEST on the horizontal peak velocity, calculations 3 and 4 (Fig. 18) are compared with DIHEST-only calculation 2a (Fig. 19). In calculation 3, the HEST and DIHEST were fired together. Thus, along the centerline of the DIHEST the peak horizontal velocities should be the same until a range of approximately 62 m (where the transition line intersects the centerline). Figure 19 shows this to be the case. At ranges where the HEST wave arrives first, the horizontal peak velocity is reduced by approximately a factor of 2 (pointed out by "precompaction" in Fig. 19). The horizontal velocity then levels off until the effects of the downstream end of the HEST appear. This type of motion suggests that the compacted material acts much like a rigid block being pushed by the DIHEST.

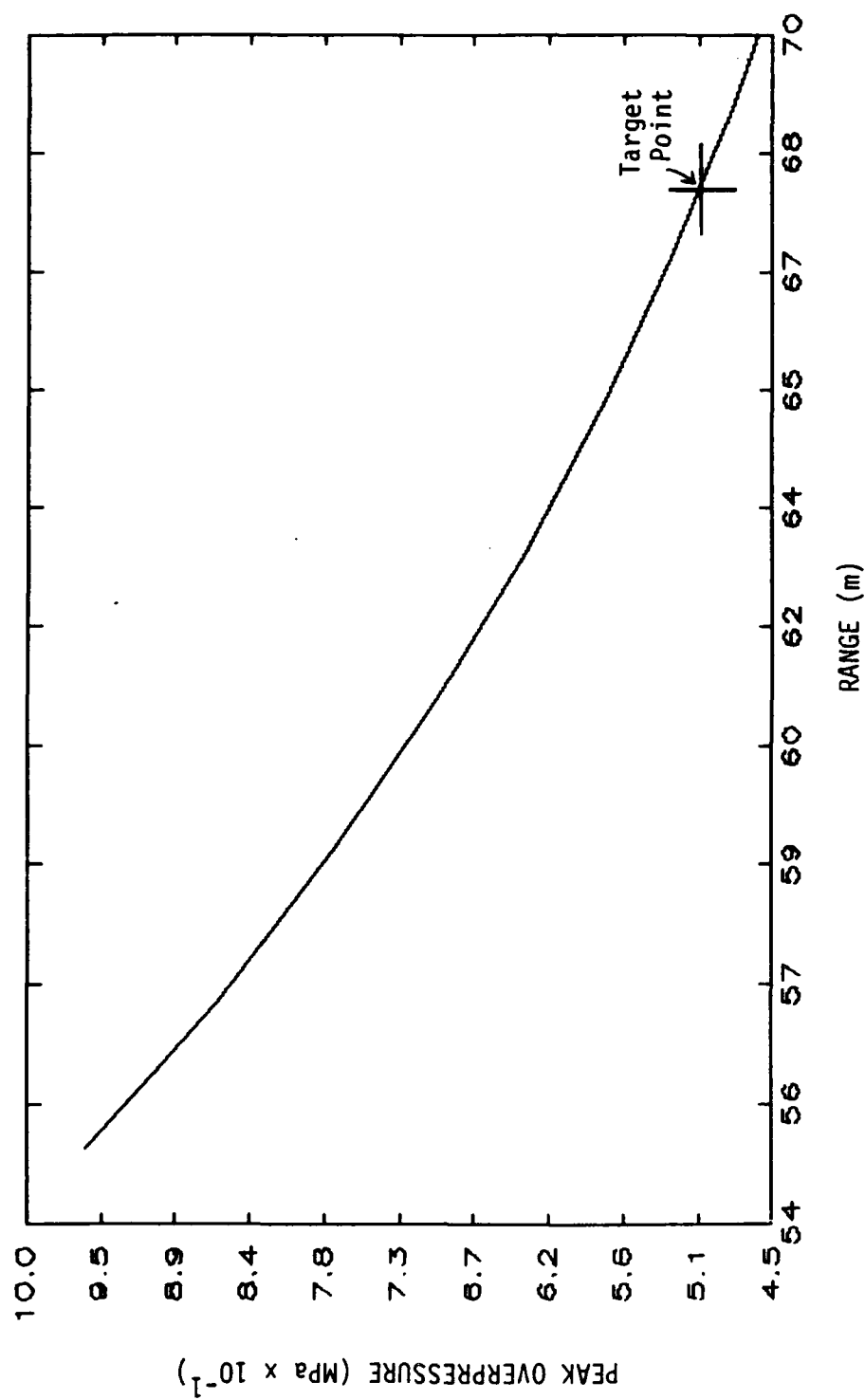


Figure 17. Peak overpressure of airblast versus nuclear range for 225-kt nuclear surface burst.

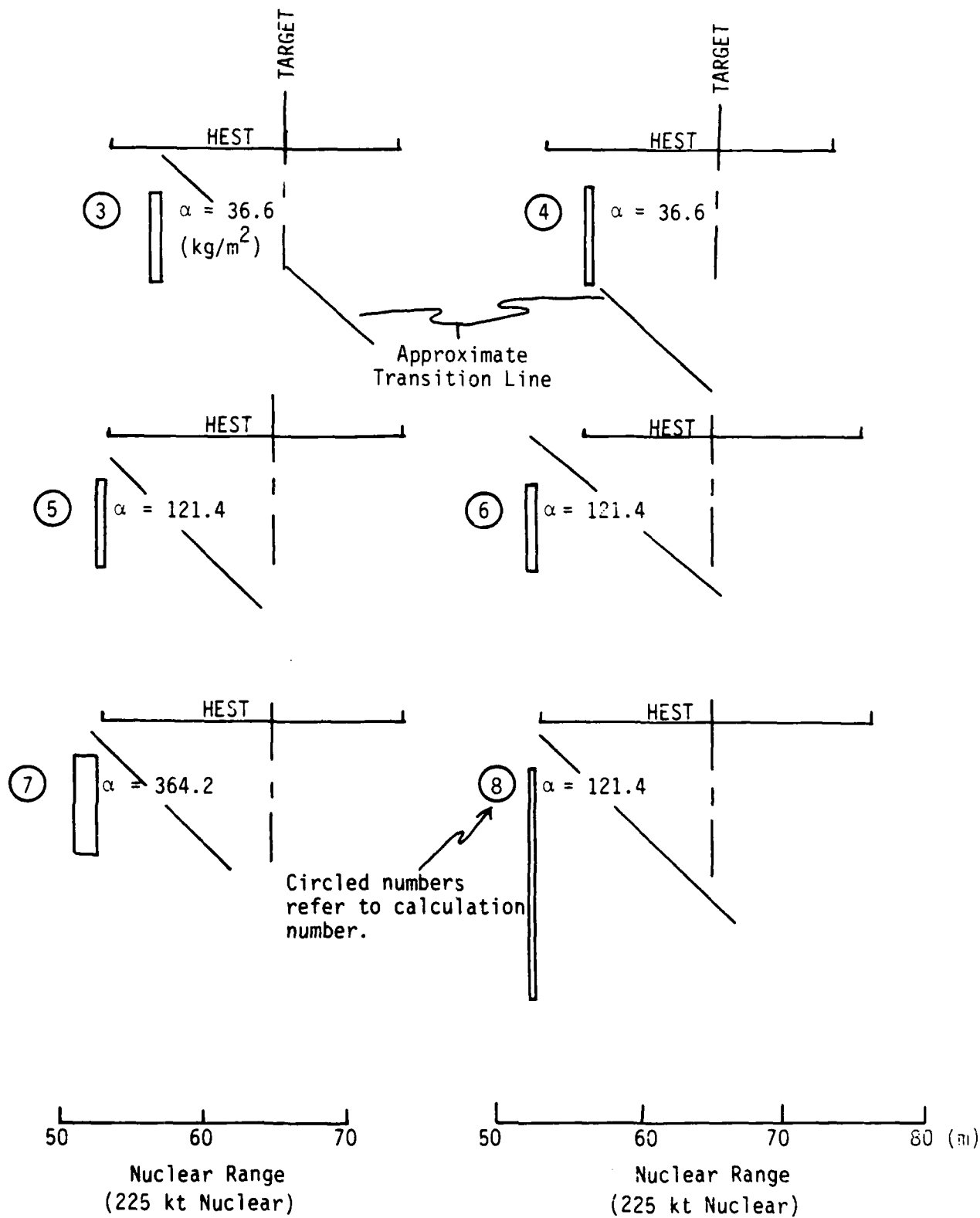


Figure 18. NMERI parametric series (Ref. 20).

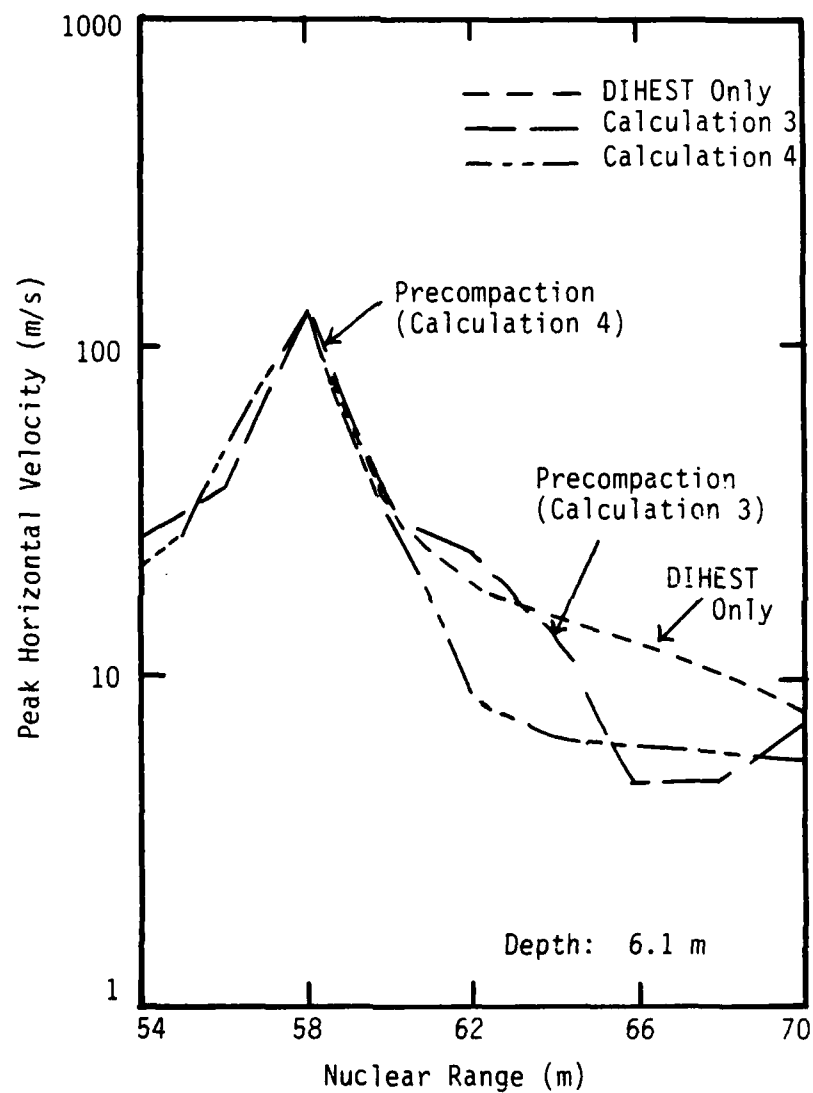


Figure 19. Comparison of DIHEST-only (dashed line) and CES calculations 3 and 4 with respect to peak horizontal velocity and DIHEST centerline.

In calculation 4, the DIHEST was not initiated until the peak velocity from the HEST reached the bottom of the DIHEST (approximately 21 ms). Thus, the motions and stresses of the DIHEST were always in a region of precompaction. Note that this situation could not be obtained in the field, as the HEST would probably destroy the DIHEST. However, it does show the limit where the DIHEST wave propagates entirely through a medium precompacted by the HEST. Close to the DIHEST, the stresses from the HEST were reduced by attenuation so that the DIHEST motions exercised new loading portions of the stress-strain curves. Although the material was affected by the HEST, stresses were sufficiently higher from the DIHEST so that the precompaction had little effect and the horizontal peak velocities behaved much like the DIHEST-only case. As the range of interest is increased, the stresses produced by the DIHEST are reduced to levels where precompaction is dominant (~60 m). At this point, the horizontal velocities begin to agree more with calculation 3. Again, the horizontal velocities appear to level out as one would expect from a rigid block.

Peak horizontal stress from the DIHEST-only (2a) case and CES 3 and 4 are shown in Figure 20. Note that near surface (1.5 m depth), the free surface in the DIHEST-only case causes the stresses to be reduced to only 3 or 4 MPa. In the case of the CES, the airblast provides the peak horizontal stresses through

$$\sigma = K_0 \sigma_z \quad (7)$$

where K_0 is the dynamic lateral earth pressure coefficient.

The σ_z is the vertical stress created by the airblast. As one progresses downward from the surface, the DIHEST-only case always has lower horizontal stresses than calculations that include an airblast simulator.

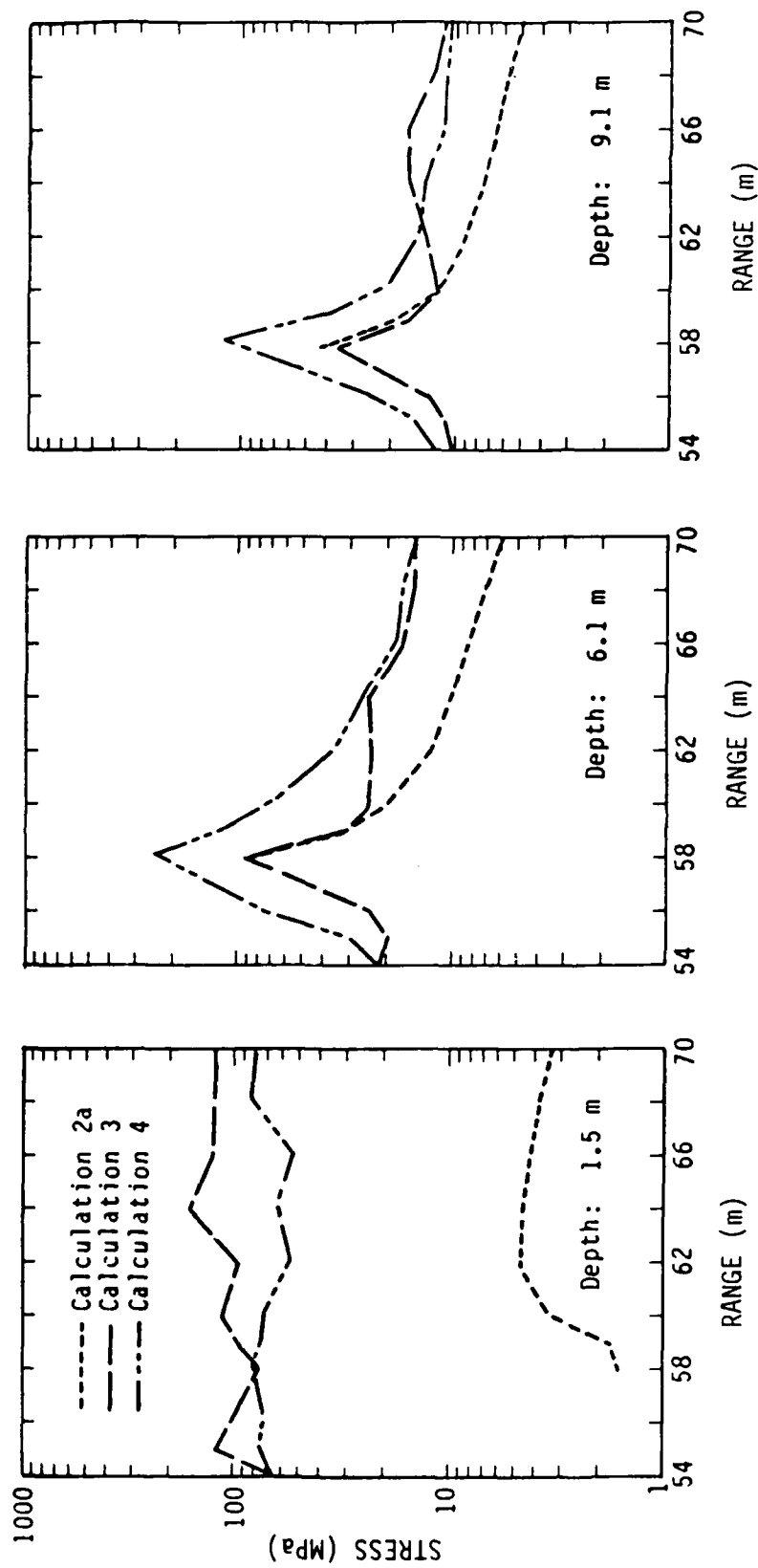


Figure 20. Peak horizontal stresses for the DIHEST-only (calculation 2a) and two CES cases (3 and 4).

Horizontal velocity waveforms from the three calculations (2a, 3, and 4) for a nuclear range of 70.0 m and a depth of 6.1 m are shown in Figure 21(a). All of the waveforms are shifted in time so that zero refers to the time of arrival (TOA) of the wave (thus, the 21-ms delay of the DIHEST in calculation 4 is not apparent). The DIHEST-only calculation (labeled "FREE") reflects a standard type of single shock that this material produces. The rise time is controlled by the difference in seismic speed versus loading velocity of the material. If TOAs were preserved, it would arrive much later than the other two waveforms. The initial arrival for calculations 3 and 4 is due to the horizontal airblast caused by the gradient of the overpressures and the nuclear sweep velocity. The DIHEST-induced wave (DI) is quite clearly isolated in calculation 4 and arrives at approximately 16 ms. Note that it adds to the horizontal airblast and appears quite different than the DIHEST-only calculation. In fact, if an estimated horizontal airblast is subtracted, the peak velocity for the added DIHEST motion would be on the order of only 3 m/s. In calculation 3, the horizontal airblast arrives at nearly the same time as the DI, and together they nearly match the peak in the DIHEST-only calculation.

Figure 21a shows some of the key aspects of the CES problems and uncertainties. First, the purely DI wave is much reduced when it encounters precompacted material. Second, the peak velocity reached is controlled by the relative timing of the airblast and DI waves. It is also clear that the DI is affected substantially by the HEST. Timing differences between the HEST and DIHEST produce substantially different shaped waveforms, implying that more than simply peaks should be used in the design of the CES simulator. Finally, these calculations show that when the DI engulfs the precompacted material, its velocity is reduced to approximately one-half the initial peak and the precompacted material of the entire test area reacts as a rigid body moving with this velocity.

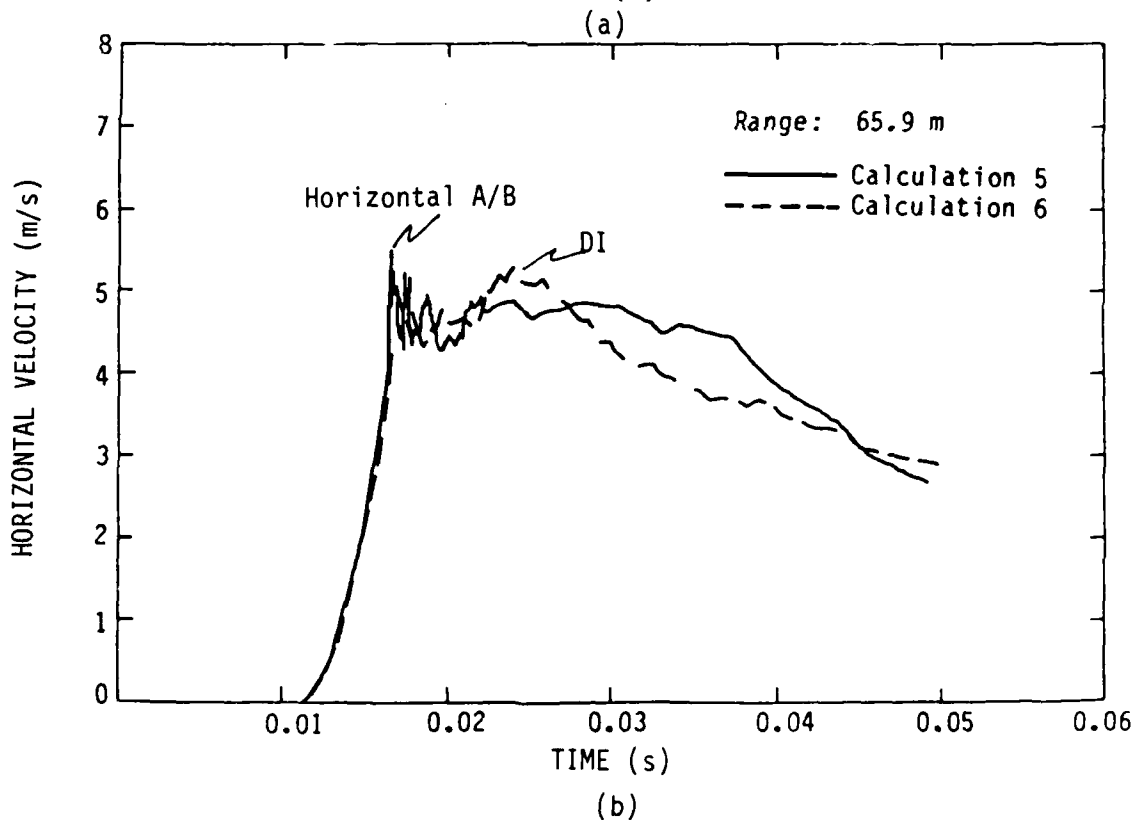
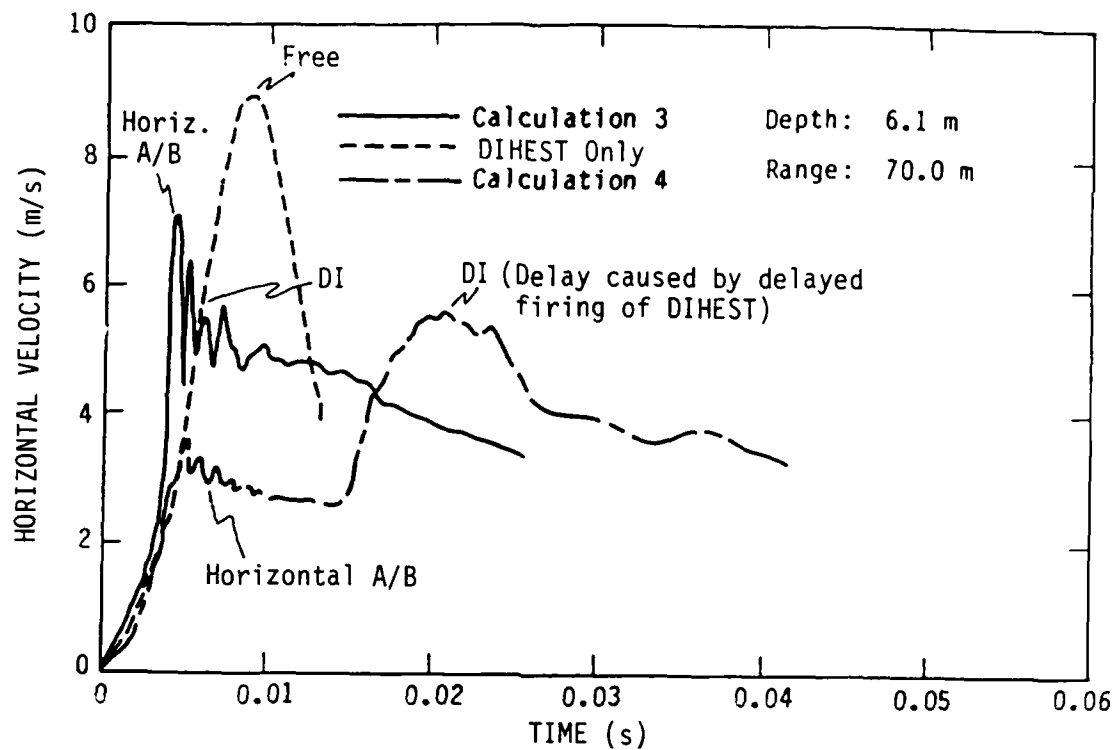


Figure 21. Comparison of waveforms for the DIHEST-only and four CES (3, 4, 5, and 16).

Limited results for calculations 5 and 6, which place the DIHEST top at the edge of the HEST (a more favorable fielding situation) are shown in Figures 21b and 22. The calculations confirm the physics seen in the previous calculations: reduction of the horizontal velocity when the precompacted material is intersected and movement of the precompacted test area material as a rigid body. The waveforms (Fig. 21b) again show the horizontal airblast and the DI. In addition, the waveforms reflect subtle changes caused by differences in timing, as the DIHEST appears to fire later than calculation 3 because of its increased distance away. We are now able to have some choice in wave shape.

Important results were obtained from calculations concerning the width (W) of the DIHEST, effects of precompaction, vertical gradients of horizontal velocities, HEST requirements, and scaling relationships in the region of 100 kt to several Mt. Initial calculations resulted in specific designs for Pre-CARES II and III, fired to test instrumentation. Using these calculations as guides, a design for CDC-1 was developed followed by CDC-2 prediction and design.

The calculations for Pre-CARES started with the initial design of the HEST, the dimensions of which were determined from relief effect considerations. Without benefit from any other studies, it appeared convenient to place the DIHEST at the edge of the HEST. The width was to be three times the height based only upon previous experience of DIHEST-only experimental data. The calculation of Pre-CARES was also simplified because the fielded DIHEST was simply a trench filled with explosive. Thus, questions are avoided about charge efficiencies used in the calculation versus those actually fielded in drill holes. The first calculation predicted horizontal velocities that were approximately a factor of 2 higher than those desired. The next calculation kept the same geometric dimensions but simply reduced

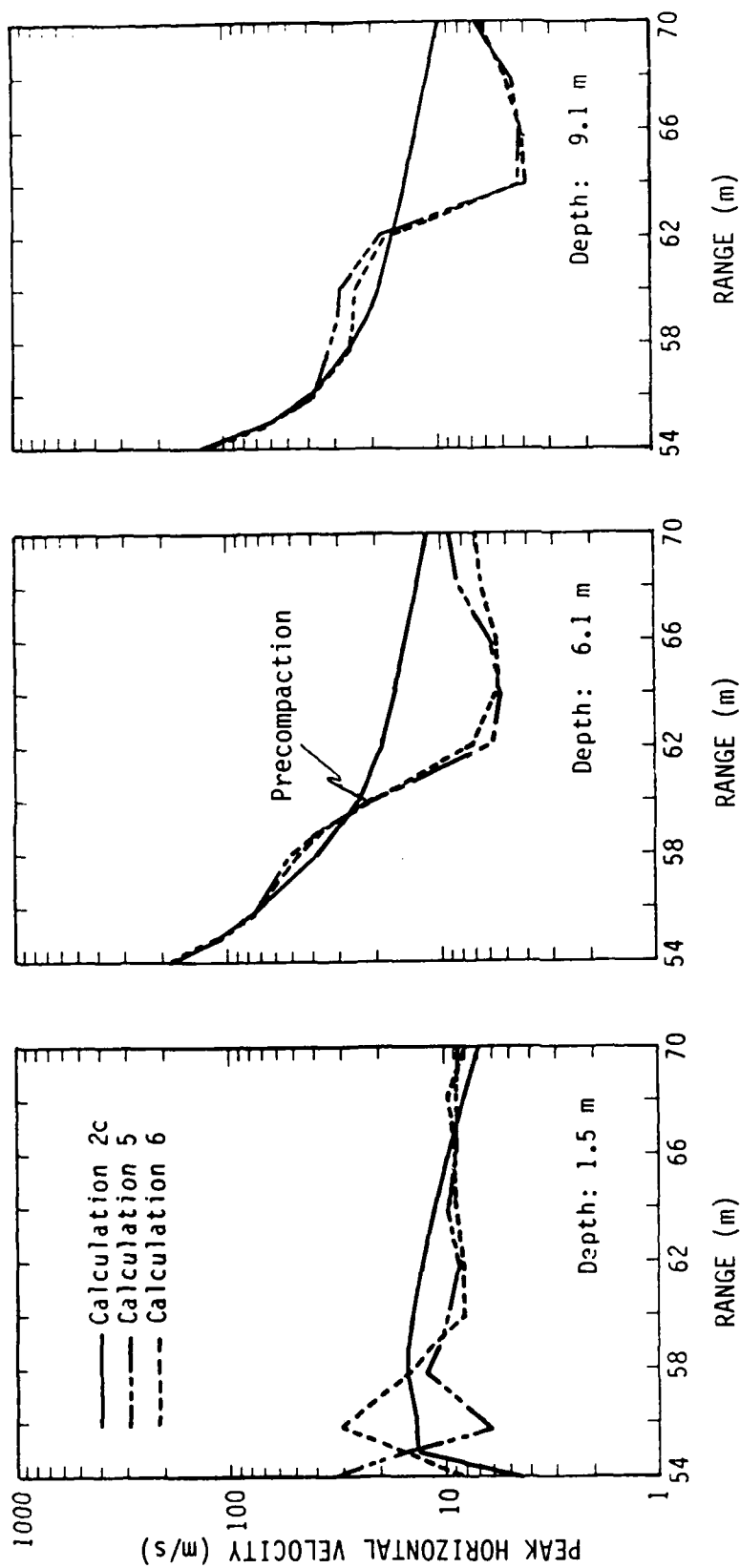


Figure 22. Peak horizontal velocities for calculations 2c (DIHEST-only), 5, and 6 (CES).

the areal density of DIHEST. The results of this calculation, presented in Figure 11, show the same phenomenology as the NMERI series; horizontal velocities follow the free-field DIHEST velocities until precompacted material is reached, at which point the velocities are reduced and the material acts like a rigid boundary.

Velocity gradients were also addressed with the Pre-CARES series. These results were shown in Figure 12. These two calculations indicated that the upper edge of the DIHEST should be near the surface and that the height of the DIHEST should be approximately twice the depth of the area of interest.

A parametric series was then conducted looking at the effects of both the lateral DIHEST placement and, more importantly, the effects of different HEST designs on the horizontal velocity produced. Questions concerning the burn rate, the required pressure gradient, and length of the HEST were answered. Figure 23 shows the results and cross sections of the modeled problem. Referring to this figure, numbers 1, 3, and 4 all used a constant pressure HEST (700 MPa) with a sweep velocity across the upper surface of approximately 7300 m/s. As shown by the horizontal velocity waveforms, few horizontal airblast-induced velocities were calculated, indicating the requirement for a pressure gradient in the HEST. The lateral position and areal density of the DIHEST were changed and showed that different arrival times of the DI wave and different amplitudes could be obtained. Doubling of the areal density essentially doubled the DI amplitude.

Calculation 2 used a variable pressure HEST that began at the DIHEST with a constant 700-MPa pressure until the predicted peak overpressure dropped below that level. The HEST then replicated the reduction given by the Brode-Speicher function. This provided an airblast-induced horizontal velocity more in

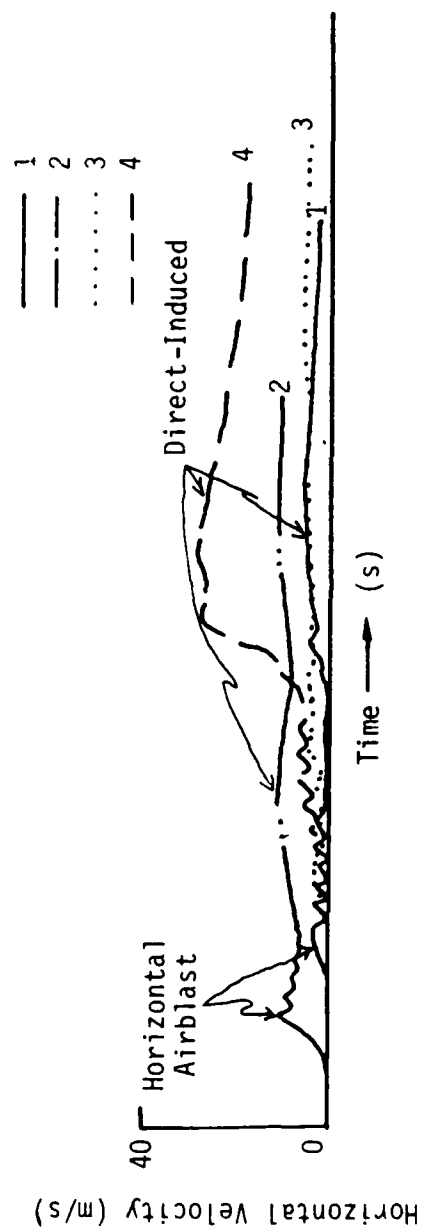
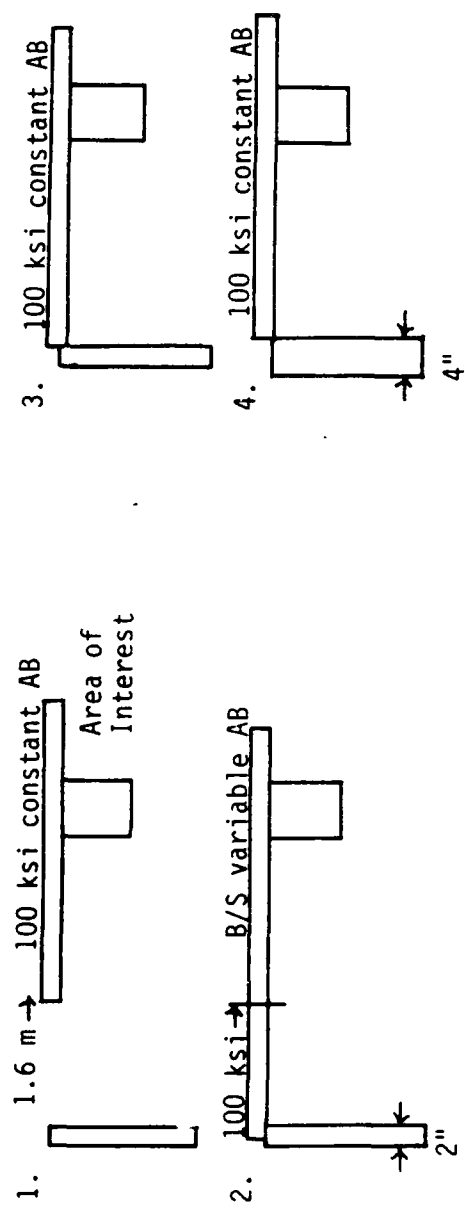


Figure 23. Parameter study for combined effects simulator.

keeping with the nuclear environment. It also indicated that, above a certain pressure, in this case 700 MPa, the airblast could be truncated to that pressure, although the CDC-1 design used 1400 MPa as the cutoff and CDC-2 tried to replicate the entire airblast.

Analysis of the Pre-CARES data indicated that the predicted velocity reduction of the DI motions was real and supported the calculations. However, the instrumentation had a high failure rate, and the data were not sufficient to completely substantiate the calculations. Posttest crater and gage surveys indicated that the crater produced by the DIHEST was indeed limited by the HEST. The crater did not intersect the target area (Fig. 24). The posttest gage survey (Fig. 24b) also showed that a DIHEST width to height ratio of 3:1 provided a usable target width of approximately W/6. Beyond that, the test-bed moved outward, parallel to the DIHEST. With this piece of information, the width of the DIHEST could be better tailored if the lateral requirements for the test area are known.

The next calculational series performed was for development of the CDC-1 simulator. The simulation criteria for both Pre-CARES and CDC-1 specified not only peak velocities, displacements, etc., but also the nuclear yield (scale) and range at which the criteria were to be met. Because both sets of criteria were based on true nuclear environments, the initial design for CDC-1 was determined by properly scaling Pre-CARES. For this problem cube-root scaling was appropriate. Thus, all linear dimensions ($L_{\text{CDC-1}}$) for the new simulator were calculated as

$$L_{\text{CDC-1}} = L_{\text{Pre-CARES}} \left(\frac{W_{\text{CDC-1}}}{W_{\text{Pre-CARES}}} \right)^{1/3} \quad (8)$$

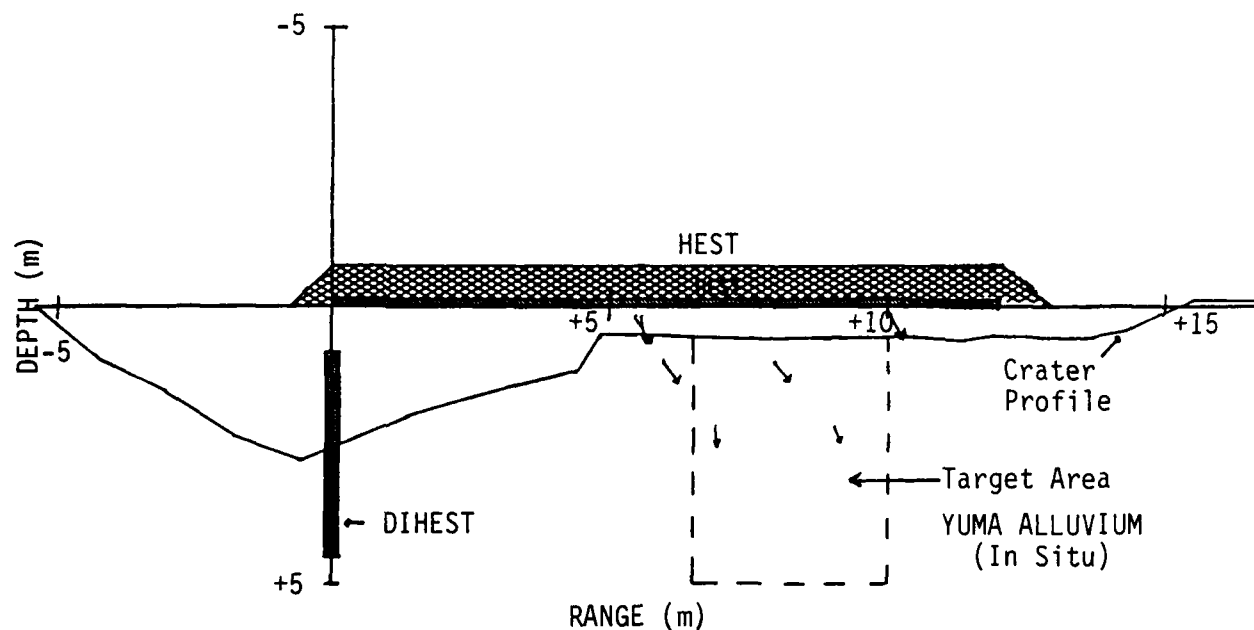


Figure 24a. Pre-CARES 2 crater profile along DIHEST centerline, and preshot and postshot gage locations for gages within 0.5 m of the centerline.

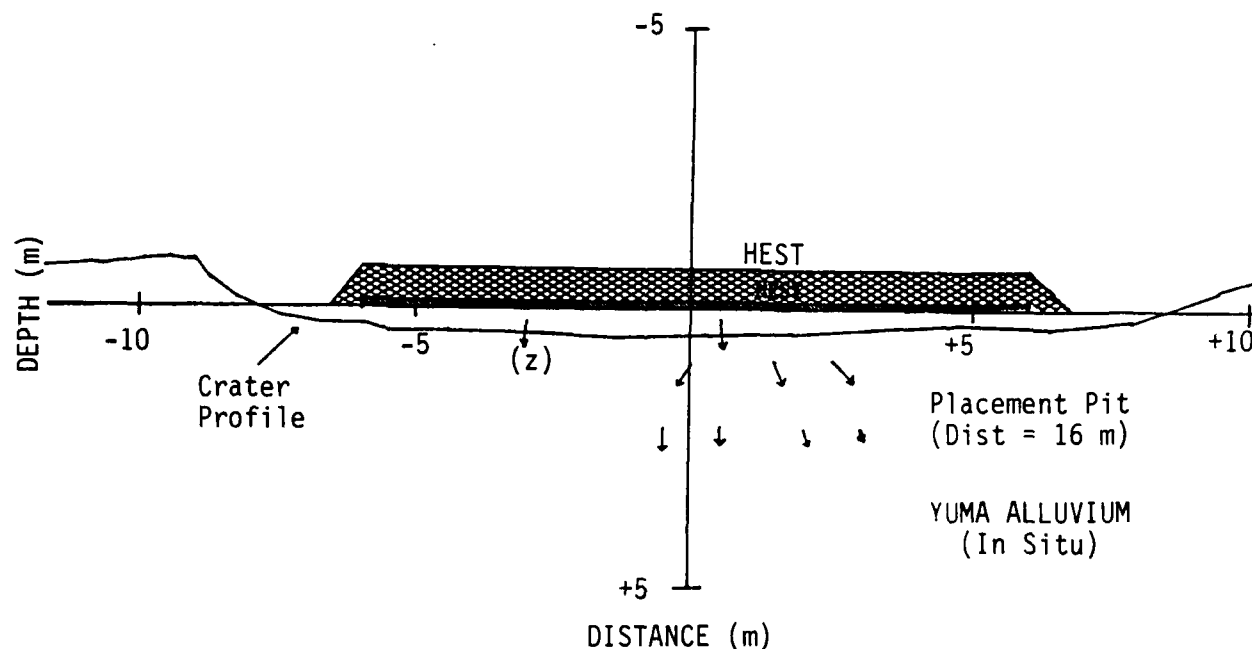


Figure 24b. Pre-CARES 2 crater profile through the HEST centerline, parallel to the DIHEST at range = 6 m, and pretest and posttest gage locations for gages within 1 m of this line.

where W is the nuclear yield. The DIHEST width and height were increased proportionately, as were the dimensions of the HEST. Note that the thickness of the DIHEST also is a linear dimension which affects the areal density, α . Thus, if the velocities were correct in Pre-CARES, then the charge density should be increased only by the cubed root of the ratio of the different yields. But CDC-1 was to use drill holes for explosive placement and the charge efficiency factor would have to be included in the calculations and accounted for in fielding.

The pretest calculation for CDC-1, used in the experiment design, simply used linear dimensions of Pre-CARES scaled by

$$L_{\text{CDC-1}} = L_{\text{Pre-CARES}} \left(\frac{12}{2} \right)^{1/3} \quad (9)$$

and an areal charge density of

$$\alpha_{\text{CDC-1}} = \alpha_{\text{Pre-CARES}} \left(\frac{12}{2} \right)^{1/3} * (\text{E.F.}). \quad (10)$$

Posttest results for horizontal velocities are shown in Figures 25 and 26. The 16-m range in Figure 16 corresponds to a nuclear range having a peak overpressure of 344 MPa (50 ksi). The scaling appeared to work well; however, the efficiency factor to convert slab explosives, used in Pre-CARES, and the calculations tended to underpredict the motions by approximately 20%. There are several other important aspects of the data and calculations that one can see from Figure 25: (1) the DI wave tends to arrive at a constant time for a specific range regardless of depth (i.e., the propagation is nearly planar in the horizontal direction); (2) the data have a more pronounced double waveform than does the calculation; (3) late-time velocities at different ranges appear to be nearly equal,

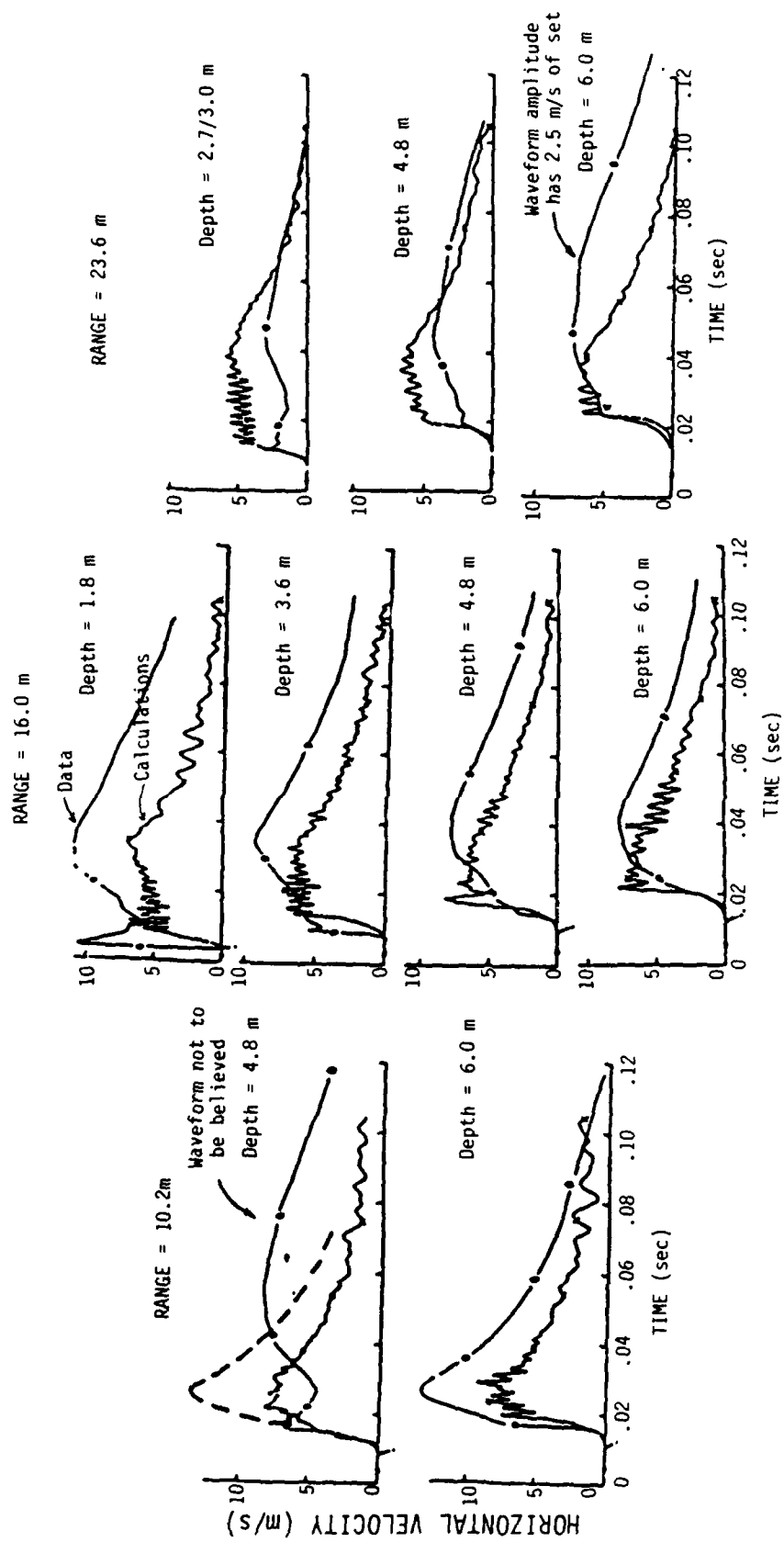


Figure 25. Horizontal velocity waveforms in the combined effects region (CDC-1).

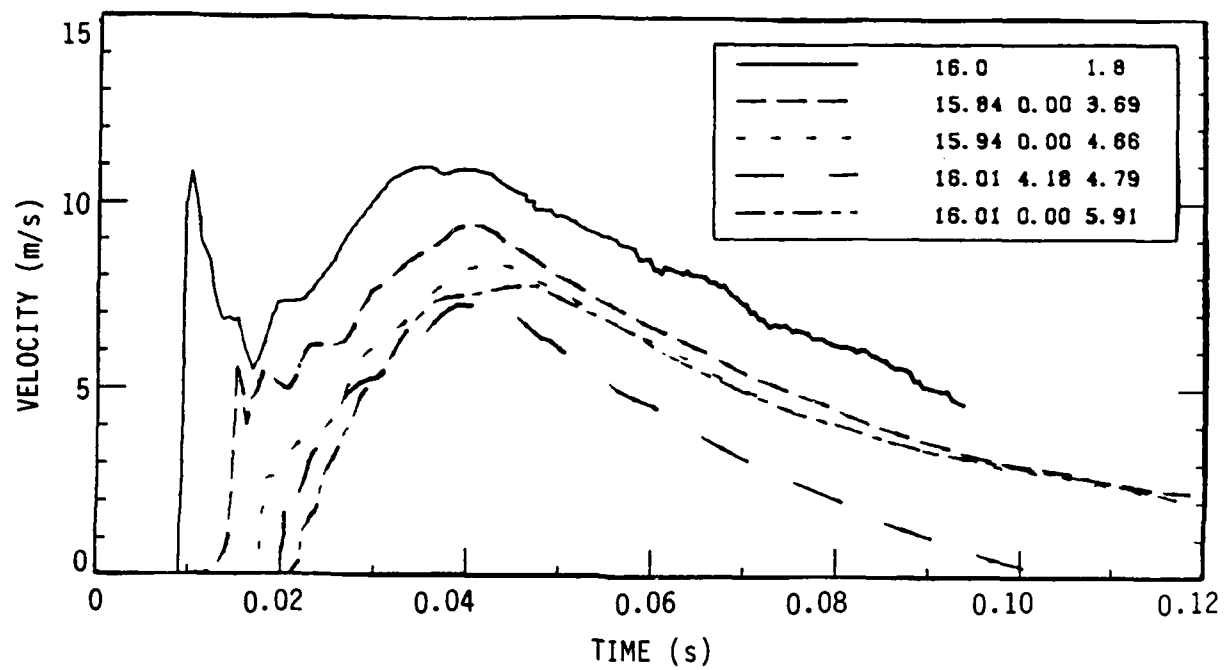


Figure 26. Horizontal velocity histories at the 16.0-m range (344 MPa) measured in CDC-1.

confirming the idea of rigid block motion of the precompacted material; and (4) both the data and calculations (Fig. 11) show very little velocity gradient in the horizontal direction (from $500 \leq P_{op} < 135$ MPa). The vertical gradient is due to the increased airblast velocity near the surface upon which the DI is added (see Fig. 26).

Crater dimensions (Fig. 27) confirm that the HEST is required to prevent cratering in the area of interest.

The design equations (not to be confused with parametric studies) give methods of extrapolating CDC-1 parameters to design other simulators fielded at similar sites with similar environments. These include:

1. Cube-root scaling of linear dimensions (lengths and areal densities) is appropriate to obtain designs for other nuclear yields.
2. Horizontal velocities have few gradients with respect to range (i.e., the rigid block idea). This implies that the simulator, although having a variable pressure HEST, actually will only simulate one specific range of interest properly. Other horizontal velocities (other overpressure ranges) should be simulated by changing the location of the area of interest (new overpressures) and altering the areal density of explosive in a linear fashion by (keeping the DIHEST in the same location)

$$\alpha_{(new)} = \alpha_{(old)} \left(\frac{v_{(new)}}{v_{(old)}} \right)$$

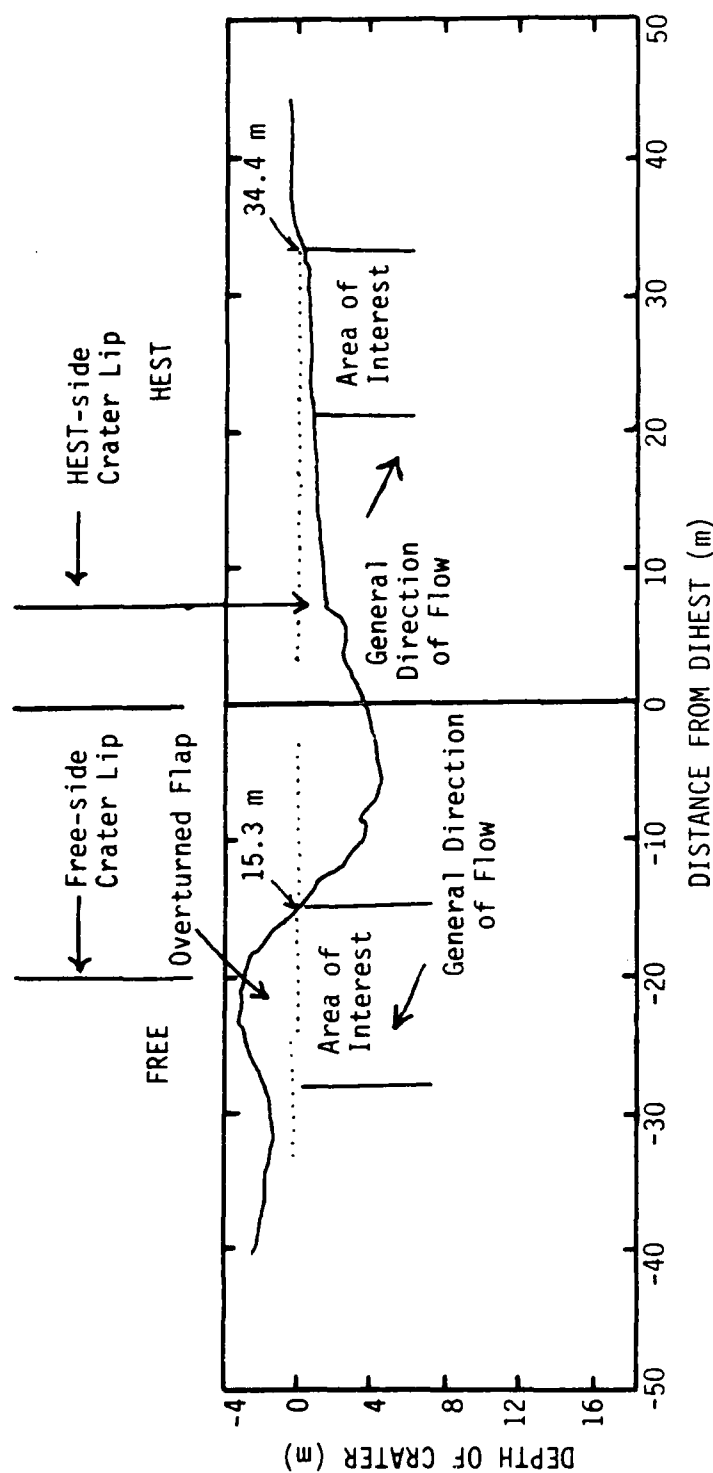


Figure 27. Cross section of the crater produced by CDC-1.

Note that this equation should also be used if new efficiency factors are required.

This methodology was used for the design and firing of CDC-2 with great success. However, if the extrapolations were too great, other factors interfered. For example, if the required overpressure was too high, then the area of interest ended up near the transition zone, perhaps intersecting it. For overpressures lower than 130 MPa (20 ksi), the timing difference between the horizontal airblast and DI might be incorrect.

EMPIRICAL RESULTS

One of the main objectives of CDC-1 was to determine the differences between the horizontal motions on the free side and combined effects side of the test-bed. From this, an empirical technique was to be developed to predict the horizontal velocities produced by a CES. The calculations suggested that the HEST would compress the material beneath, and the crater-related motion would propagate as a reload wave through this precompacted material. Where the DIHEST arrived first, beneath a transition line, the HEST would propagate as the reload wave; above that line the crater-related would propagate as a reload wave.

Because of reloading characteristics, calculations suggested DIHEST velocities and displacements would be substantially less than predicted by Drake's equation (Eqns. 2, 3, and 4). In summary, the data show that the effect of the HEST was not as great as that calculated; however, there was a detectable difference. The peak velocities produced by the DIHEST are lower by 40% or so from the free-field DIHEST data. The measured peak displacements were, however, larger than the pretest calculation by 100%. In addition, the calculation showed a blending of horizontal airblast with the DI which was not observed in the data.

To understand how waves integrate with each other, an attempt was made to separate the waveforms from the data (airblast and DI) and directly address the differences. The approach was to define a horizontal airblast-only wave shape from both the data and calculations. This wave shape was then normalized to the actual airblast peak and subtracted from the total horizontal waveform. By doing this a generalized prediction procedure using superposition was developed.

Figure 28 shows four waveforms, two from the free side of the test and two from the CES side. With the exception of the 10-m free-field wave, all are direct reproductions of the CDC-1 data. The waveform at 10 m is interpolated from other real data at different ranges. The horizontal velocity waveforms from the CES side are direct reproductions and contain both the airblast and DI motions. Conclusions made are:

1. In all cases the combined effects waveform attains a lower peak velocity than the DIHEST-only wave.
2. Overall wave shapes are different. The free-field DI resembles what one would expect from a concave up-loading curve with seismic toe (e.g., a seismic toe arrival, concave to the left wave shape, and a lagging peak). On the other hand, the combined effects waveform appears concave downward on rise--opposite to the free-field side one. This implies that the material model is much stiffer on loading than the free-field side. After initial loading, softening is seen, resembling an unload/reload stress-strain curve. In addition, the combined effects wave peaks at an earlier time than the free-field implying a much faster "loading" velocity.
3. The combined effects horizontal velocity wave represents a maximum, because any airblast-induced motions must be subtracted from the DI.

Range = 10.0 m
Depth = -4.8 m

Range = 16.0 m
Depth = -4.8 m

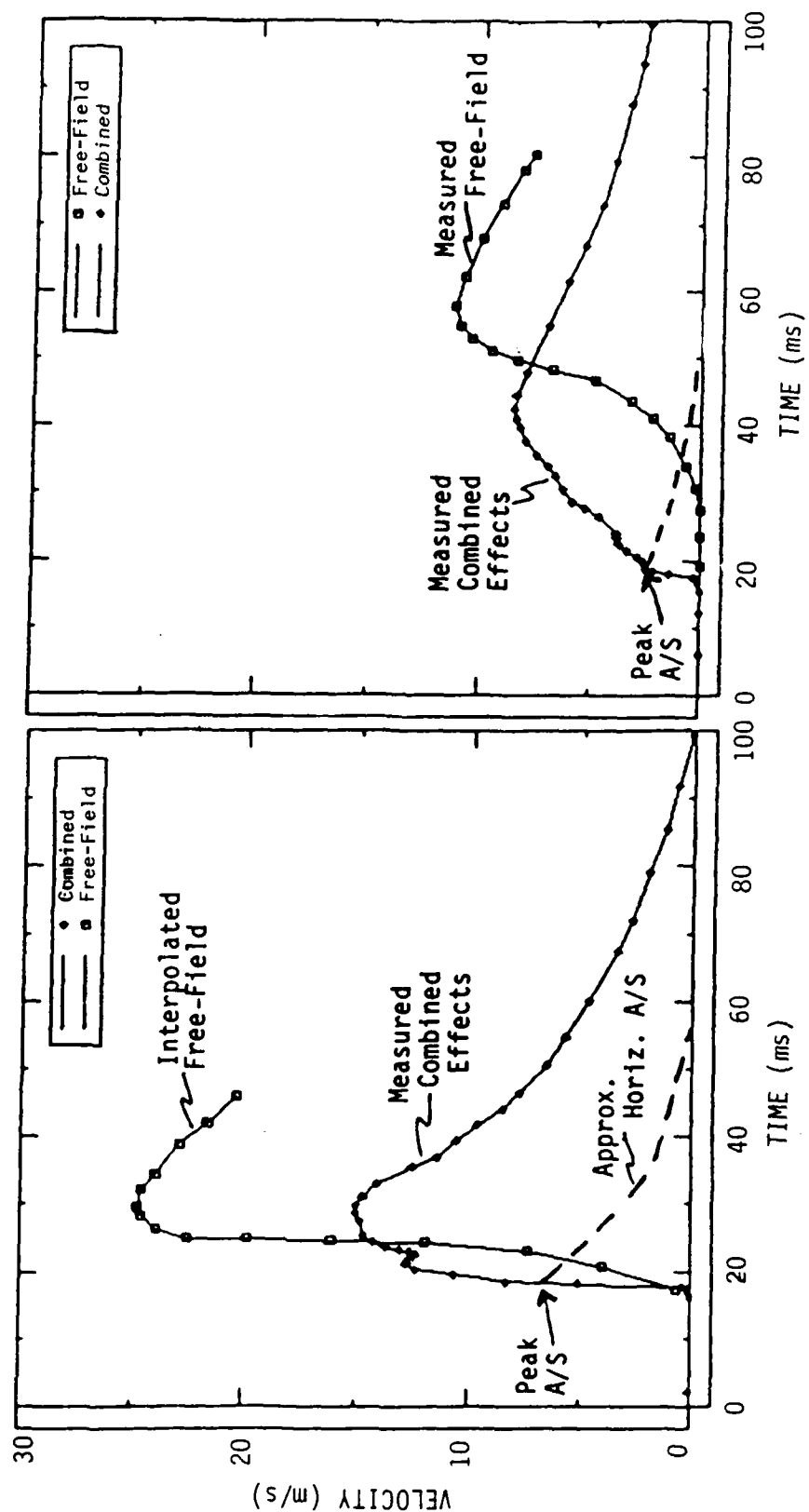


Figure 28. Waveform comparison of unHSTed and HESTed velocity waveforms.

From the way the waves are delivered in the region of interest--first the airblast followed by the direct-induced, it would seem reasonable that there are basically two waves superposed. First the airblast wave exercises the virgin stress-versus-strain loading curves. Following that, the CR wave propagates through exercising the reload/unload curves. The pretest calculations show that the airslap causes the largest peak stresses; and the DI stresses are relatively low, resulting in the CR truly reflecting the unload/reload curve. Active stress gages in the test confirm the calculations.

Alluvium is a highly nonlinear and nonelastic material, especially when subject to a single cycle loading. However, after the first initial loading, subsequent loadings are along a very stiff, nearly linear-elastic reload curve. This allows the use of superposition of waves after initial crush-up, or in this case, airblast loading. Thus, airblast unloading and DI loading can be superposed. It also implies that DI loading in the combined effects region is along a substantially different path than initial loading.

Consider a cross section of the CES as presented in Figure 29. (This is a key to developing a more general prediction technique for a CES.) Considering a more global field and working from the extreme far field inward (right to left in Fig. 29), the effects of the two simulators become more obvious. Because the HEST is basically directed downward, little of its energy will be observed at ranges greater than C. Thus, for ranges greater than this, Equations 2-4 could be used for prediction of the DIHEST, as its stress wave will be propagating in a region unaffected by the HEST. In the same vein, motions from the DIHEST will be unaffected by the HEST in areas to the left and beneath the transition line shown in the figure. These also can be predicted using Equations 2-4.

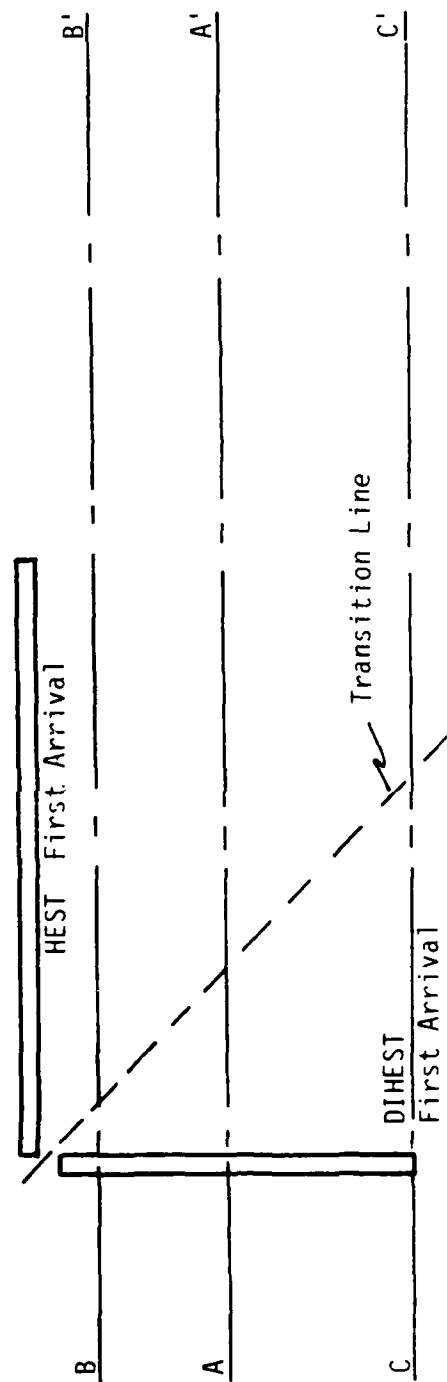
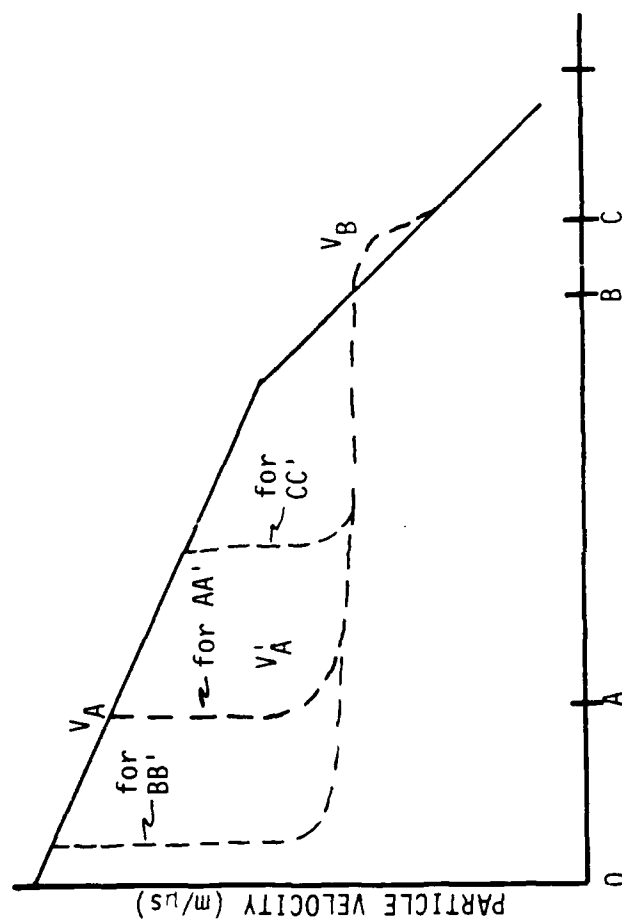


Figure 29. CES cross section and resulting peak DIHEST velocities.

The calculations show that when the DIHEST wave interacts with the HEST motions, the velocities are affected. In dry material, the calculations show that the horizontal velocity is initially reduced by approximately one-half, and the material then reacts like a rigid block whose velocity is determined by the DIHEST charge used and the effects of the compaction. Considering that at some point, C, the free-field DIHEST motions are again reached, this would imply the horizontal velocity achieved at the transition zone is nearly a constant until point C. This effect is also seen in Figure 19, where the location of the transition zone determines where initial horizontal velocity reduction occurs; but when it does occur the velocity is reduced to a more or less constant value. In Figure 29, velocity reduction for lines AA', BB', and CC' would occur at different ranges, but they would all be reduced to a similar value.

Figure 30 shows this from the CDC-1 data. The total horizontal waveforms, two of which are shown in Figure 28, have had the horizontal airslap component subtracted, and the resulting peaks are plotted in Figure 30 along with the free-field DIHEST. The prediction curve in Figure 30 was developed in a manner described for Figure 29. The data from CDC-1, also shown in Figure 30, appear to substantiate the method for dry material. Thus, the procedure would include determination of the free-field DIHEST-only motions, the determination of the transition zone, the knowledge of the extent of the HEST, and the effect of the precompaction of the HEST on the DIHEST motions.

To illustrate the procedure further, consider the ACID combined effects simulator (Figs. 3 and 4) in corresponding detail. Figure 31 shows a schematic cross section of the ACID test with representative peak horizontal velocity and displacements. The HEST and DIHEST were fired simultaneously and the DIHEST motions acted as if they were DIHEST only until the ground shock came near the HEST. The motions of the HEST also

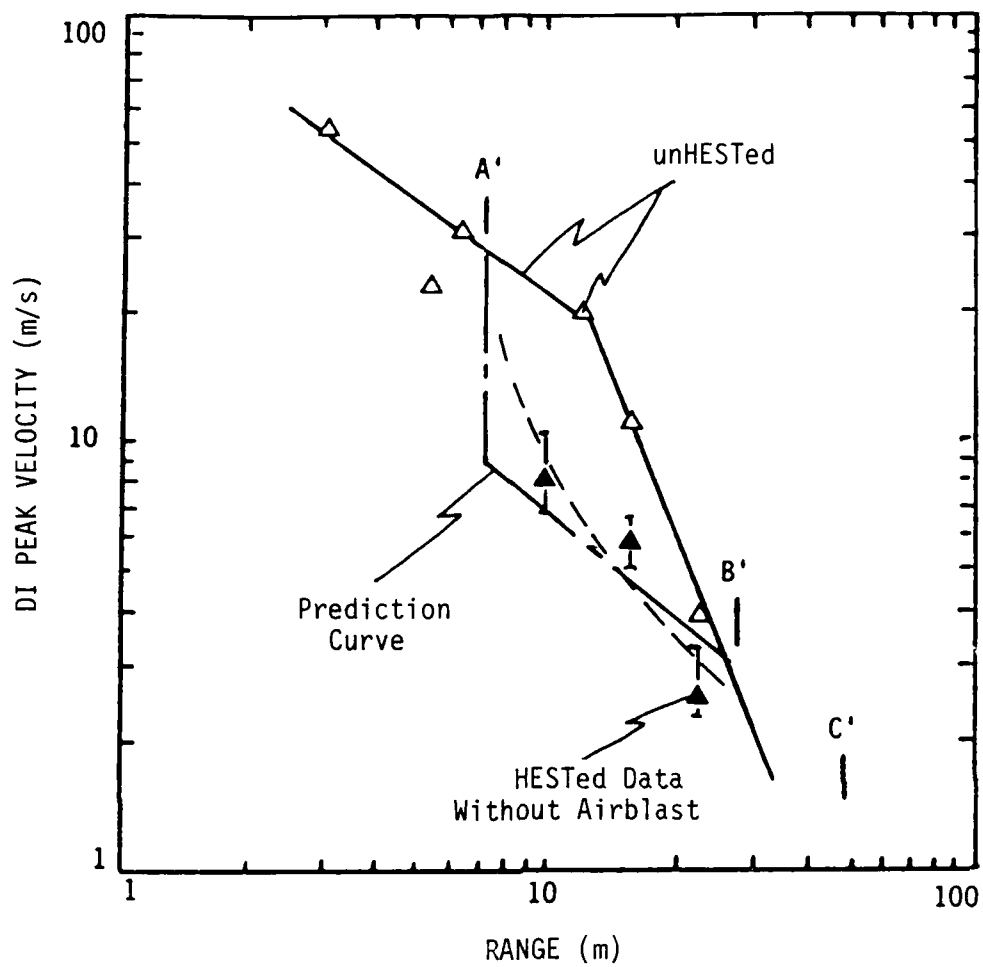


Figure 30. Comparison of peak velocities of the DI wave with airblast subtracted.

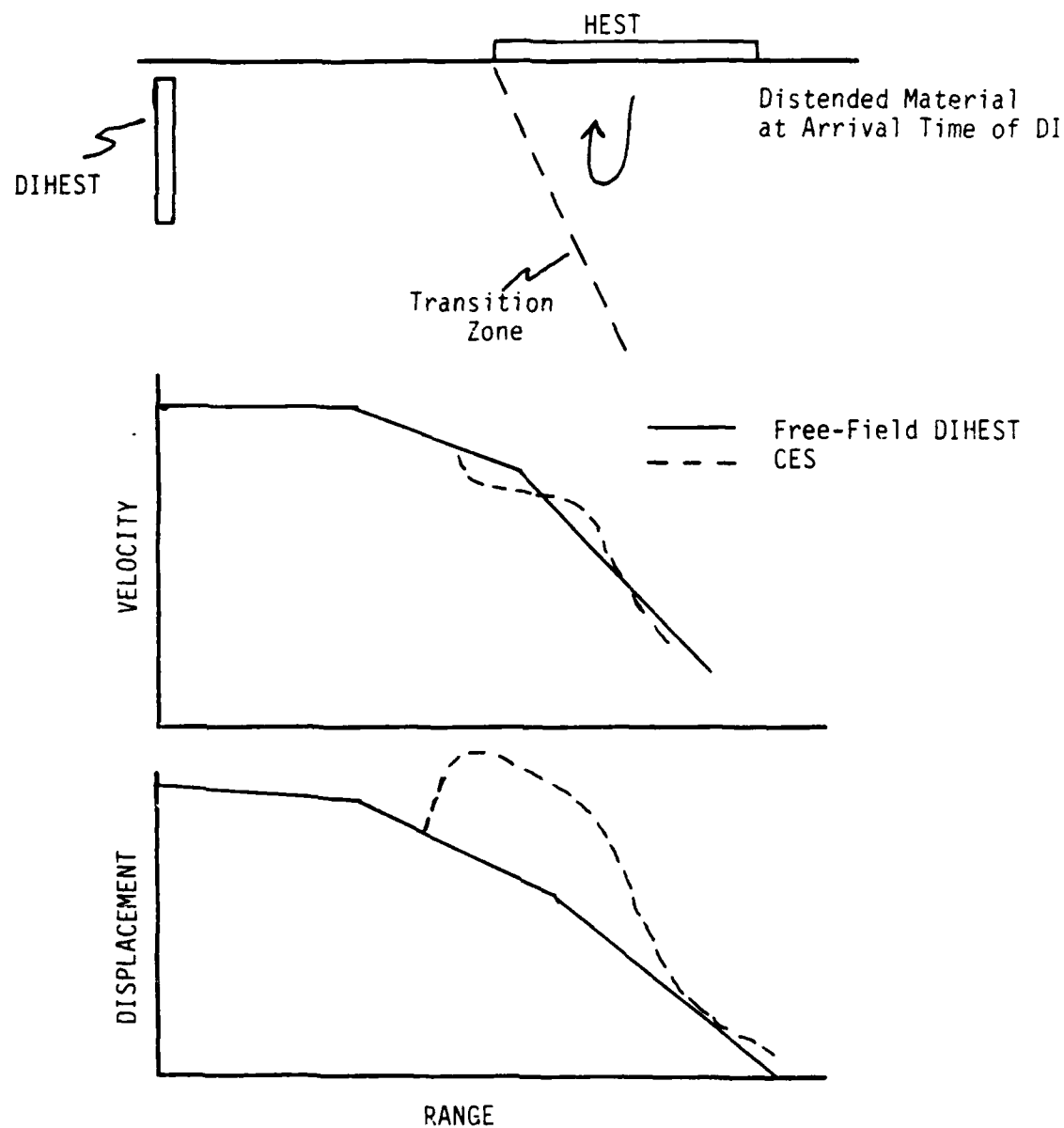


Figure 31. ACID Test (compare with Fig. 3).

were unchanged until the DIHEST motions approached. The HEST produced initial crush-up and precompaction as in the CDC series. However, because of the small size of the HEST, before the DIHEST shock arrived, the HEST produced edge effects that left the material in a distended state. The transition zone was now established and surrounded the entire HEST test-bed. The DIHEST motion, when arriving at the transition zone, were modified, in this case by increasing displacements. This illustration shows qualitatively the same basic principles of combining the two simulators, but the effects of precompaction are much different.

Both previous examples were for dry alluvial materials. For a homogeneous wet site, similar arguments could be used in developing a CES. The major difference is the effect of precompaction of the wet material on the DIHEST motions. The wet material, at these pressures, remains essentially elastic, and simple superposition of the two simulators would be a plausible first approximation. Unfortunately, neither free-field design equations for DIHEST or HEST are readily available for wet material. Calculations would therefore be required.

The design technique described above would not lend itself well to a CES in a layered site of wet and dry materials. The nuclear environment for such a site would be very complicated. The amplitude and arrival times of various waves is a complicated interaction of geology and material properties. The nuclear environment would have to be studied carefully and each prominent feature of the waveforms would probably be generated by a separate part of the CES. The design would depend heavily on calculations.

OUTSTANDING TECHNICAL ISSUES

Two unresolved issues remain when designing a CES at a scale larger than 96 kt for a dry Yuma-type site. The first issue relates to the large quantities of explosives required for the full-scale DIHEST. The HEST is of little concern because tests such as LS-1 and LS-2 have been successfully fired at large scales. However, the design of the CDC-2 DIHEST has been essentially the largest test yet fired. The second concern is that of instrumentation, its survival of the larger full-scale displacements, and long duration recordings.

The suggested depth of the DIHEST for proper simulation is to be approximately twice the depth of interest of the test area. For a 30-m-deep silo, suggested are DIHEST drill holes on the order of 60 m. At this depth, a hydrostatic head of approximately 1.4 MPa (200 psi) would exist. Data for the equation of state for the appropriate explosives (e.g., ANFO or nitromethane) that are generally used do not exist for these high static pressures. Because of this, it is difficult to estimate precisely the output from the DIHEST charges. The increased static pressures would tend to increase the explosive densities and detonation velocities. The final design and criteria for CDC-2 expected ground motions to be within 20%, which required rather well-known explosive characteristics. Before a full-scale CES is designed, a simple single-hole calibration test with full-scale dimensions and simple instrumentation would be required.

In both CDC-1 and CDC-2, long-term motion measurements were hampered by displacement related cable failures and long-term accelerometer baseline shifts. In addition, the frequency resolution of many gages required for simulator diagnostics was limited by the long cable runs to the recording trailer required by the large quantities of high explosive.

At full-scale, the displacements will be even larger than those experienced in CDC-2 for the same depths of burial used for protection. Although usually considered an engineering problem, careful thought must be given to the gage placement and cable routing to assure survivability. In both tests, failures were abundant at discontinuities in the cabling protection. Where stainless steel tubing was joined to nylon tubing or where the tubing ended, there were numerous failures on both CDC-1 and CDC-2. Flexible tubing (either nylon or reinforced rubber) seemed to perform best. Discontinuity in cabling must be avoided.

The cable runs for CDC-2 were approximately 2 km in length. The length for a larger scale simulator would be simply cube-root scale of the smaller scaled distance. For a 500-kt surface burst simulator, a run of approximately 3.4 km would be required. By using hardened digital records that do not require operators during the shot, cable length could be greatly reduced. It appears that a switch to the digital systems is essential at full scale.

Long-term baseline shifts remain a problem without an obvious solution. On the one hand, larger scales will tend to produce lower accelerations that should improve the ratios between initial peaks and late-time dwells. On the other hand, the larger scales will require longer duration recordings of the data. Perhaps new types of gages can be used; however, they do not appear forthcoming in the near future. Perhaps different recording methods, with the possible introduction of white noise to increase the dither factor (Ref. 21), could be investigated. At this time no clear avenue of approach is available.

SUMMARY OF DESIGN PROCEDURES

INTRODUCTION

A design methodology has been developed by understanding in detail one experimental series--CDC. Calculational parametric studies, pretest predictions, and test data analysis have all led to one specific design set. This set may be used as a basis for designs of combined effects simulators for dry material, near-surface velocity-time histories for ranges corresponding to 500 to 140 MPa (80 to 20 ksi) peak overpressures of nuclear yields ranging from 2 to 225 kt. Conceptual design layouts for other yields, ranges, and geologies could be estimated, but to assure correct simulation the designs must be calculated. The requirement for calculational support cannot be overemphasized. This section will consider the procedure to be used with specific requirements where known. It is basically a summary of preceding discussions.

STEP 1. THE NUCLEAR CRITERIA

A determination of the nuclear environment is a prerequisite to any design. Also required are the criteria that the final simulator must meet. By understanding the environment, the individual parts of the simulator can be determined. In the case of dry material, the airblast is replicated with a high explosive airblast simulator: HEST, BLEST, HIFI HEST, STABS, or a combination thereof. These designs are well known. Dry material also produces a rather simple crater-related (CR) velocity history that can be well simulated with only a DIHEST. Although not calculated, other homogeneous sites (dirt and rock) would produce nuclear motions that could be replicated with similar configurations. Layered sites are not well understood and additional calculations are required at this time for construction of a simple design, although global designs similar to CARES have been used.

STEP 2. THE PARTS REQUIRED

For dry material (and usually for homogeneous wet and rock material), the CES should consist of a HEST and/or BLEST having variable overpressures and a single DIHEST. Tests to date indicate that the DIHEST should be placed at the leading edge of the HEST. Other arrangements could be considered, but this is the only CES configuration proven through actual tests.

STEP 3. GEOMETRICAL LAYOUT

For design of a CES in dry material, the following dimensions have been tested and appear adequate for a motion simulator. Stresses at peak horizontal velocities are not replicated well. Calculations of edge relief effects indicate that the HEST should extend from $5.2 \text{ m/kt}^{1/3}$ ($\sim 2760 \text{ MPa}$) to $17.6 \text{ m/kt}^{1/3}$ (68 MPa) nuclear range for a simulation of approximately $4 \text{ ms/kt}^{1/3}$ at the 344-MPa (50-ksi) range of interest. The $12.4 \text{ m/kt}^{1/3}$ lateral extent of the HEST should be moved so that the center of the HEST is approximately over the overpressure of interest. This size is expected to give good vertical motion and vertical stress simulation to the bottom of a generic missile structure (full scale of 30 m). If more simulation time is required, the HEST should be made larger; however, care must be taken not to exceed the nuclear dimensions of the problem.

The DIHEST is located at the leading edge of the HEST at a depth of $0.6 \text{ m/kt}^{1/3}$ beneath the surface. Small adjustments to this depth are appropriate. The height of the DIHEST should be approximately twice the depth of the area of interest. The width of the simulator should be between three and four times the height.

Extension of this design in dry material to pressures lower than approximately 100 MPa should be done with care and

additional calculations. As was shown with the ACID data (24 MPa), the HEST may become so small that the DIHEST is no longer directly beneath the HEST, resulting in a decoupling of the two simulators.

In wet or rock material, the edge effects may travel at velocities substantially greater than at a dry site, resulting in rather large HEST dimensions. A simple calculation for a range corresponding to 550 MPa (80 ksi) in wet material indicates a HEST that includes nuclear ground zero--clearly questionable. These kinds of uncertainties must be worked out before any new designs are attempted.

STEP 4. EXPLOSIVE ESTIMATES

Explosive estimates for the HEST are given in Figure 8 for initial estimates. (Since the HEST is a pressure boundary adjustment for different material types is not expected for these initial estimates.) Details of specific designs for the HEST should be a result of 1-D calculations.

Using the dimensions listed above for the DIHEST, a horizontal velocity of 7 m/s (344-MPa overpressure) should be produced with an areal density of $5.3 \text{ kg/m}^2 \cdot \text{kt}^{1/3}$ of explosive placed in drill holes located at the edge of the HEST. Adjustments to new velocities are direct and adjustments to new yields are through cube-root scaling.

REFERENCES

1. Babcock, S.M. Combined DIHEST Calibration (CDC-1) Test, AFWL-TR-86-79, Air Force Weapons Laboratory, Kirtland AFB, NM, To Be Published.
2. Schuster, S.H., A.V. Cooper, and F.M. Sauer, Air Force Manual for Design and Analysis of Hardened Structures, AFWL-TR-87-57, Air Force Weapons Laboratory, Kirtland AFB, NM, To Be Published.
3. Sanai, M., "Simulation Development for Silo Test Program (STP)," Final Report on Contract DNA001-82-C-0103, SRI International, Menlo Park, CA, March 1984.
4. Wampler, H.W., G. Leigh, M.E. Furbee, and F.E. Seusy, "A Status and Capability Report on Nuclear Airblast Simulation Using HEST," Proceedings of Nuclear Blast and Shock Simulation Symposium, 28-30 November 1978, DNA Report 4797, Vol. 1, GE Tempo, DASIAC, Santa Barbara, CA, November 1978.
5. Taylor, H.R. and D.C. Phillips, Design and Construction Test Facility to Simulate the Effect of a Nuclear Detonation (Rock Test I), AFWL-TR-69-7, Air Force Weapons Laboratory, Kirtland AFB, NM, June 1969.
6. McGrath, F.G., HARD PAN I Test Series, Vol. 1, Test Plan, AFWL-TR-75-249, Air Force Weapons Laboratory, Kirtland AFB, NM, October 1975.
7. Parsons, R., E. Rinehart, and K. Benson, ACID Test: Simulation and Technology Development, AFWL-TR-79-199, Air Force Weapons Laboratory, Kirtland AFB, NM, June 1982.
8. Henny, R., Personal Communications, Air Force Weapons Laboratory, Kirtland AFB, NM, 1986.
9. Rinehart, E.J. and G.M. Lloyd, "EZ-3 Pretest Prediction: Part I - The Free Field," CRT-TR-3852-2, California Research and Technology, Inc., Albuquerque, NM, 1986.
10. Higgins, C.J., R.L. Johnson, and G.E. Triandafilidis, "The Simulation of Earthquake-Like Ground Motions with High Explosives," Final Report #CE-45(78)NSF-S07-10, University of New Mexico, Albuquerque, NM, 1978.
11. Babcock, S.M., Combined DIHEST Calibration (CDC-2) Test, AFWL-TR-87-97, Air Force Weapons Laboratory, Kirtland AFB, NM.

REFERENCES (Continued)

12. Foster, R.C., J.M. Thomsen, G.M. Lloyd, and R.R. Franzen, "A Modal Analysis Routine for Calculations and Data," CRT-TR-3760-2, California Research and Technology, Inc., Pleasanton, CA, 1986.
13. Drake, J.L., "Consistent Scaling of DIHEST Ground Motions," ASH Simulation Working Group Meeting, 28-29 August 1984, Applied Research Associates, Vicksburg, MS, 1984.
14. Sanai, M., "Simulation Development for CDC-1 and CDC-2 Combined Effects Simulators," SRI Final Report to CRT, Subcontract 3760-01-85, California Research and Technology, Inc., Pleasanton, CA, July 1986.
15. Rinehart, E.J., "Shear Wave Generation of Near-Surface Spall," Journal of Geophysical Research, Vol. 90, No. 136, pp. 4567-4576, 1985.
16. Shinn, J.D., Relief Effects Beneath Nuclear Airblast Simulators Conducted Over Dry Alluvial Soils, AFWL-TR-83-31, Air Force Weapons Laboratory, Kirtland AFB, NM, 1983.
17. Thomsen, J.M., et al., "DIHEST Test Design and Prediction for the DDT-1, DDT-2 and WES-X Tests," CRTN784-01PM, California Research and Technology, Inc., Pleasanton, CA, July 1984.
18. Dobratz, B.M., "Properties of Chemical Explosives and Explosive Simulants," LLNL Explosive Handbook, UCRL-52997, Section 8, Lawrence Livermore National Laboratory, Livermore, CA, March 1981.
19. Thomsen, J., E. Rinehart, S. Ruhl, and F. Sauer, "DIHEST Calibration Test No 1. Preliminary Technical Test Plan," CRTN-3760TP1, California Research and Technology, Inc., Dublin, CA, January 1985.
20. Babcock, S.M., P.S. Bacon, and D.K. Rudeen, Parametric Calculations Investigating a Combined HEST/DIHEST Simulator, AFWL-TR-86-65, Air Force Weapons Laboratory, Kirtland AFB, NM, November 1985.
21. Schuchman, L., "Dither Signals and Their Effect on Quantization Noise," IEEE Transactions on Communication Technology, pp. 162-165, December 1965.

END

DATE

FILMED

9-88

DTIC